

Weakly bound nuclei:

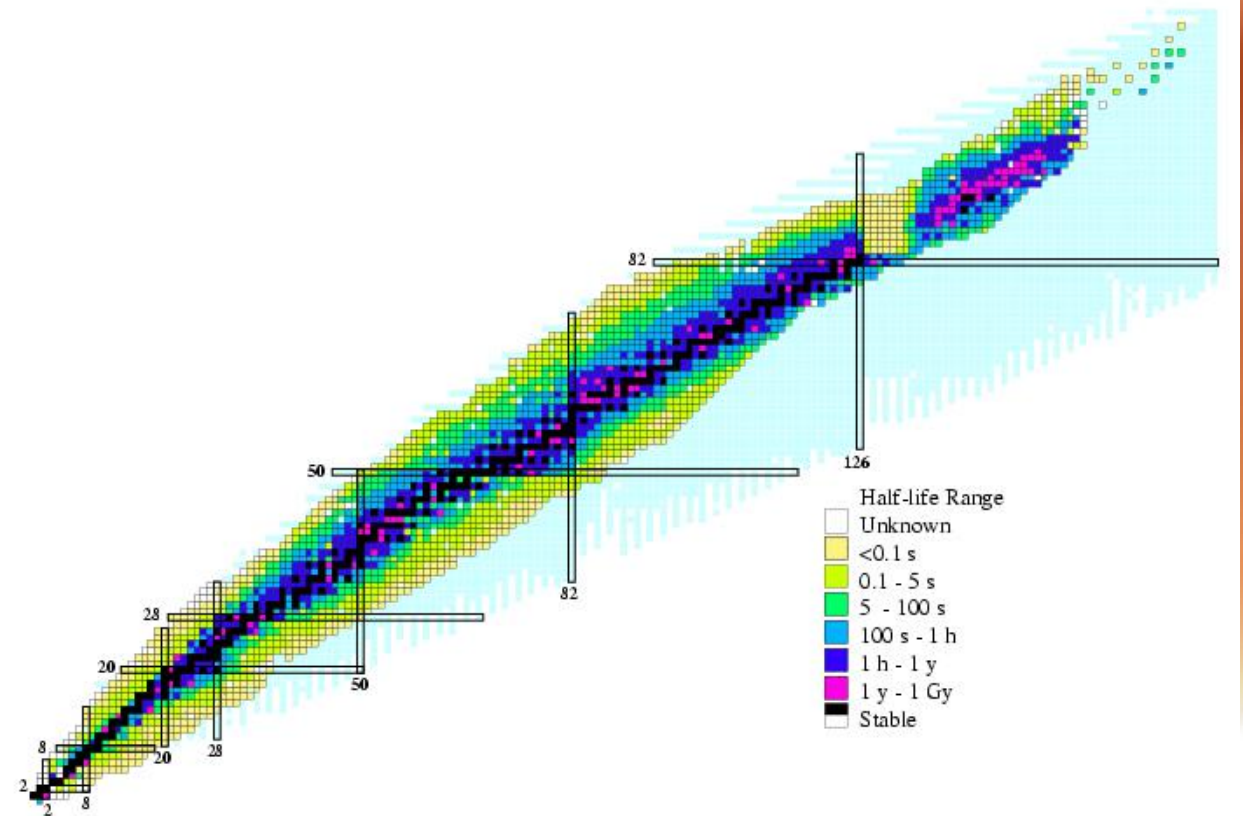
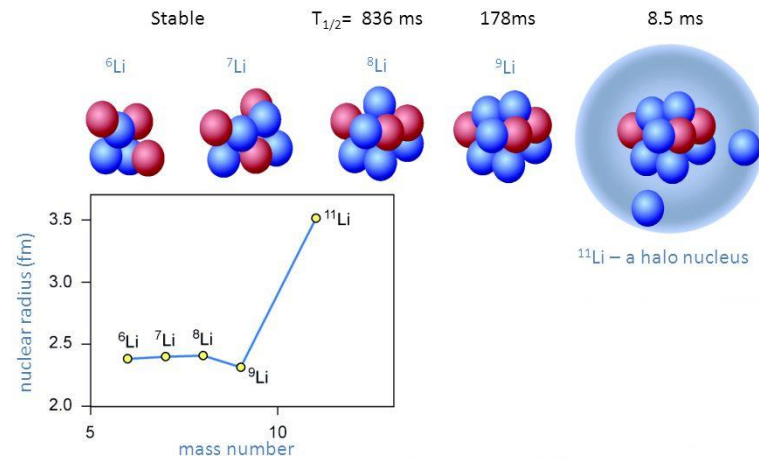
A unified description of intrinsic and relative degrees of freedom

Weakly bound nuclei:

A unified description of intrinsic and relative degrees of freedom



Bound lithium isotopes

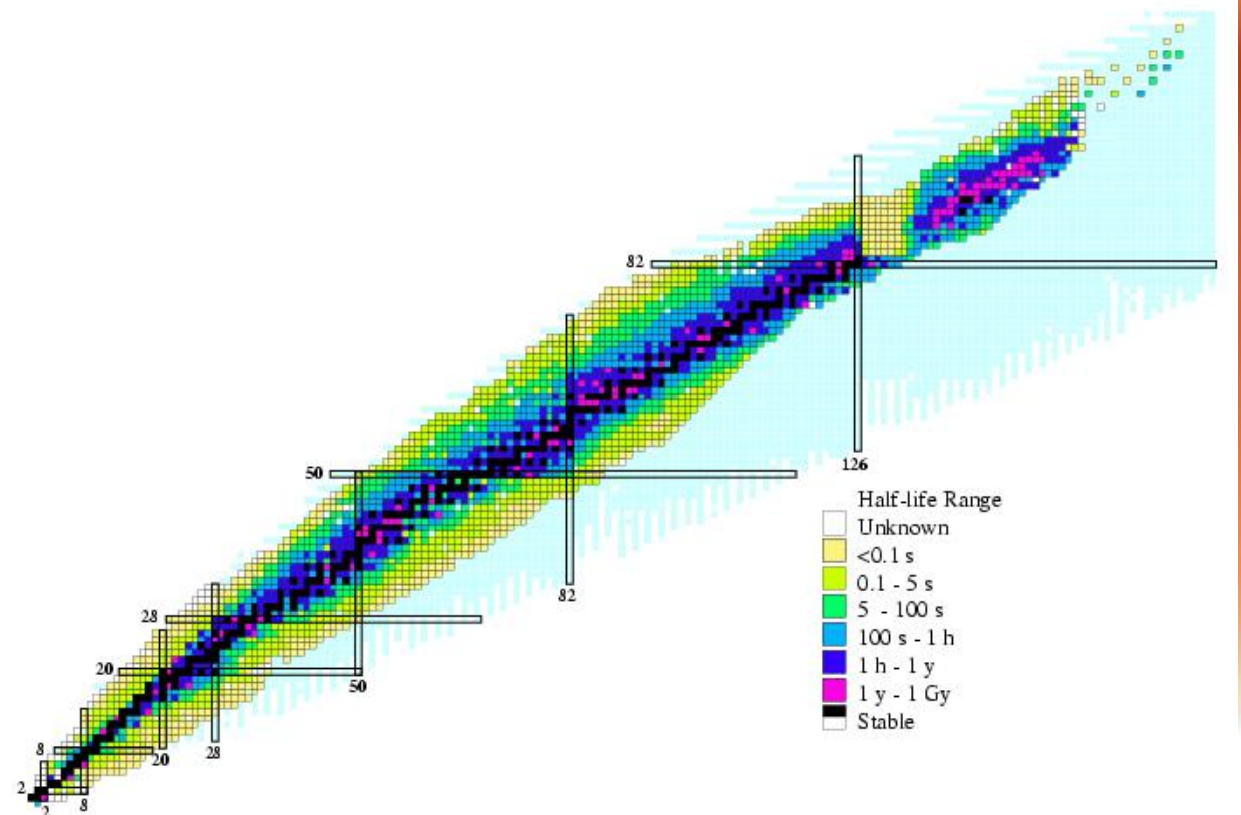
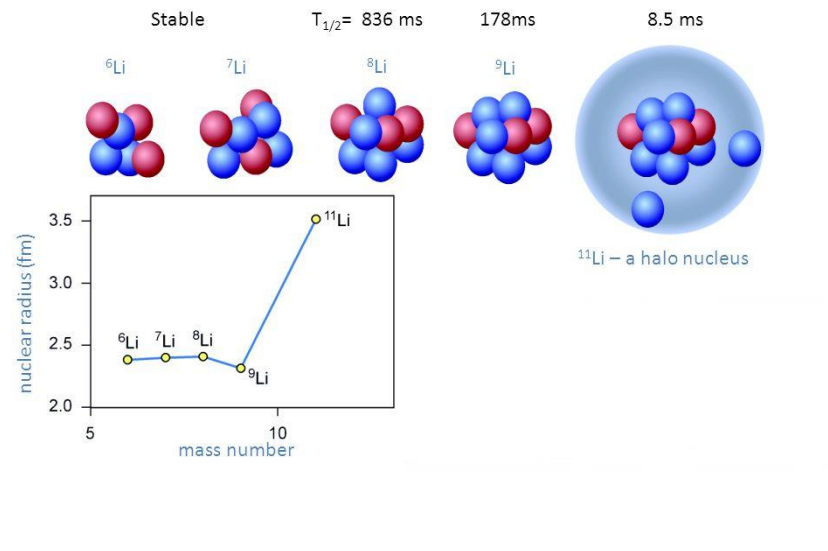


Weakly bound nuclei:

A unified description of intrinsic and relative degrees of freedom



Bound lithium isotopes

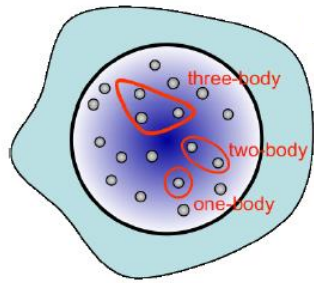


$$[T_x + T_y + V_{12}(r_{12}) + V_{13}(r_{13}) + V_{23}(r_{23})] \Psi = E\Psi$$

- ✓ The core is assumed to be an inert particle.
- ✓ What to do when experimental information is not available.

Weakly bound nuclei:

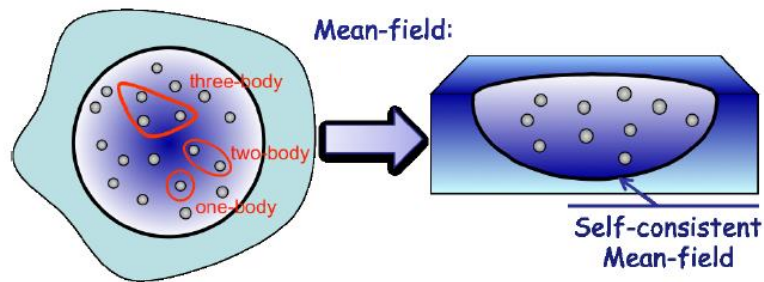
A unified description of intrinsic and relative degrees of freedom



$$H = \sum_i T(i) + \sum_{i < j} V^{(2)}(i, j) + \sum_{i < j < k} V^{(3)}(i, j, k)$$

Weakly bound nuclei:

A unified description of intrinsic and relative degrees of freedom



"Simple" Trial state:

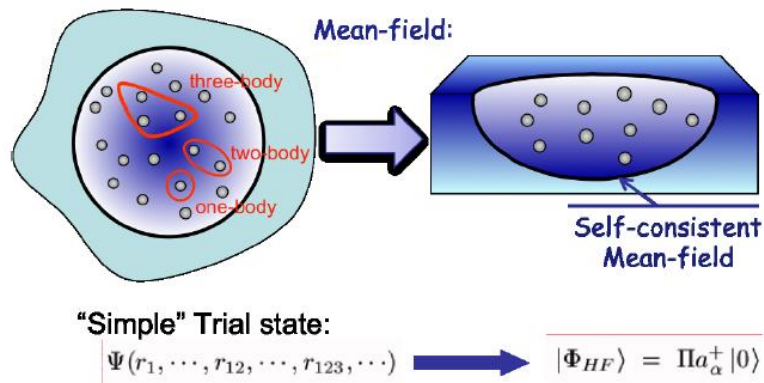
$$|\Psi(r_1, \dots, r_{12}, \dots, r_{123}, \dots)\rangle \longrightarrow |\Phi_{HF}\rangle = \Pi a_\alpha^\dagger |0\rangle$$

$$H = \sum_i T(i) + \sum_{i < j} V^{(2)}(i, j) + \sum_{i < j < k} V^{(3)}(i, j, k)$$

- ✓ The particles do not interact with each other, but through an average mean-field.
- ✓ The complex N-body wave function is replaced by a Slater determinant.

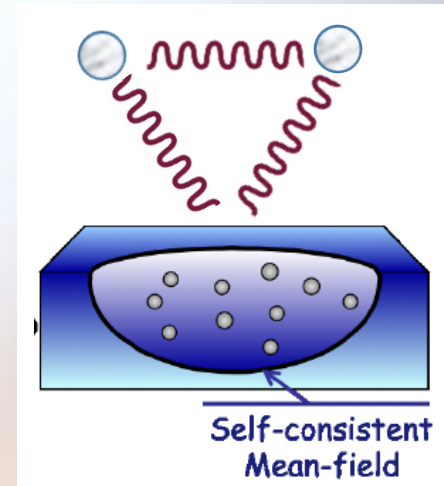
Weakly bound nuclei:

A unified description of intrinsic and relative degrees of freedom



$$H = \sum_i T(i) + \sum_{i < j} V^{(2)}(i, j) + \sum_{i < j < k} V^{(3)}(i, j, k)$$

- ✓ The particles do not interact with each other, but through an average mean-field.
- ✓ The complex N-body wave function is replaced by a Slater determinant.



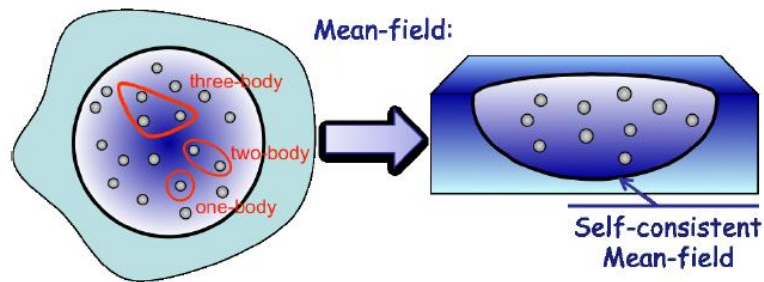
- ✓ The mean-field determines the interaction with the loosely bound nucleons.



Three-body problem

Weakly bound nuclei:

A unified description of intrinsic and relative degrees of freedom

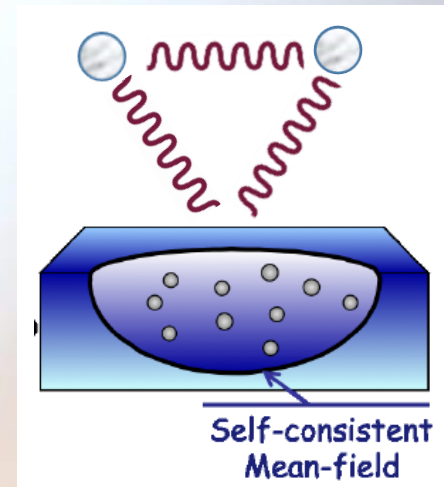


"Simple" Trial state:

$$|\Psi(r_1, \dots, r_{12}, \dots, r_{123}, \dots)\rangle \longrightarrow |\Phi_{HF}\rangle = \Pi a_\alpha^\dagger |0\rangle$$

$$H = \sum_i T(i) + \sum_{i < j} V^{(2)}(i, j) + \sum_{i < j < k} V^{(3)}(i, j, k)$$

- ✓ The particles do not interact with each other, but through an average mean-field.
- ✓ The complex N-body wave function is replaced by a Slater determinant.



- ✓ The mean-field determines the interaction with the loosely bound nucleons.



Three-body problem

- ✓ The presence of the loosely bound nucleons distorts the mean-field.

- ✓ The distorted mean-field modifies the core-nucleon interaction and the wave function of the valence nucleons.

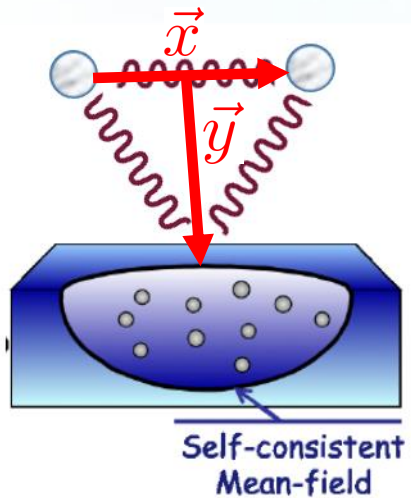
Self-consistent calculation

Weakly bound nuclei:

A unified description of intrinsic and relative degrees of freedom

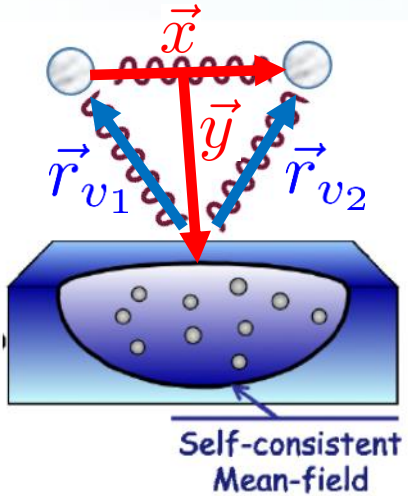
- ✓ Some formal hints about the formalism
- ✓ The case of ^{26}O
- ✓ Proton dripline: ^{70}Kr
- ✓ Approaching the dripline: Ca isotopes
- ✓ Summary and possible extensions

Formalism:



$$H = \underbrace{\frac{1}{4mA} \sum_{i=1}^A \sum_{j=1}^A (\vec{p}_i - \vec{p}_j)^2 + \sum_{i < j}^A V_{ij}}_{H_c} + \underbrace{\frac{p_x^2}{2\mu_x} + \frac{p_y^2}{2\mu_y} + V_{v_1 v_2}}_{H_3} + \underbrace{\sum_{i=1}^A (V_{iv_1} + V_{iv_2})}_{H_{coup}}$$

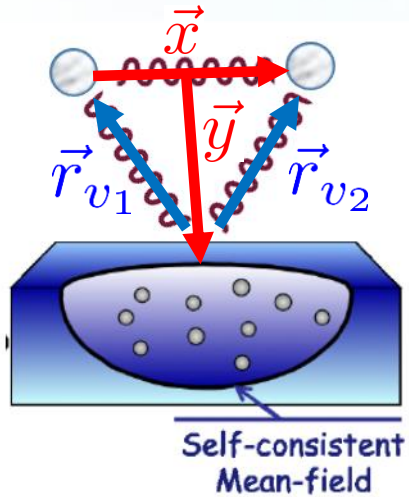
Formalism:



$$H = \underbrace{\frac{1}{4mA} \sum_{i=1}^A \sum_{j=1}^A (\vec{p}_i - \vec{p}_j)^2 + \sum_{i < j}^A V_{ij}}_{H_c} + \underbrace{\frac{p_x^2}{2\mu_x} + \frac{p_y^2}{2\mu_y} + V_{v_1 v_2}}_{H_3} + \underbrace{\sum_{i=1}^A (V_{iv_1} + V_{iv_2})}_{H_{coup}}$$

$$\begin{aligned} \Psi &= \mathcal{A} \{ \Phi_c(\{\vec{r}_A\}) \psi_3(\vec{r}_{v_1}, \vec{r}_{v_2}) \} \\ &= \Phi_c(\{\vec{r}_A\}) \psi_3(\vec{r}_{v_1}, \vec{r}_{v_2}) - \sum_{i=1}^A \Phi_c(\vec{r}_{v_1}, \{\vec{r}_{A-1}\}) \psi_3(\vec{r}_i, \vec{r}_{v_2}) \\ &\quad - \sum_{i=1}^A \Phi_c(\vec{r}_{v_2}, \{\vec{r}_{A-1}\}) \psi_3(\vec{r}_{v_1}, \vec{r}_i) + \sum_{i < j}^A \Phi_c(\vec{r}_{v_1}, \vec{r}_{v_2}, \{\vec{r}_{A-2}\}) \psi_3(\vec{r}_i, \vec{r}_j) \end{aligned}$$

Formalism:

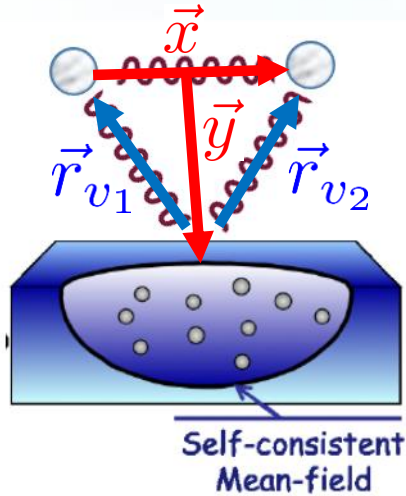


$$H = \underbrace{\frac{1}{4mA} \sum_{i=1}^A \sum_{j=1}^A (\vec{p}_i - \vec{p}_j)^2 + \sum_{i < j}^A V_{ij}}_{H_c} + \underbrace{\frac{p_x^2}{2\mu_x} + \frac{p_y^2}{2\mu_y} + V_{v_1 v_2}}_{H_3} + \underbrace{\sum_{i=1}^A (V_{iv_1} + V_{iv_2})}_{H_{coup}}$$

$$\Psi = \mathcal{A} \{ \Phi_c(\{\vec{r}_A\}) \psi_3(\vec{r}_{v_1}, \vec{r}_{v_2}) \}$$

$$E = \langle \Psi | H | \Psi \rangle = \langle \Phi_c | H_c | \Phi_c \rangle + \langle \psi_3 | H_3 | \psi_3 \rangle + \langle \Psi | H_{coup} | \Psi \rangle$$

Formalism:



$$H = \underbrace{\frac{1}{4mA} \sum_{i=1}^A \sum_{j=1}^A (\vec{p}_i - \vec{p}_j)^2 + \sum_{i < j}^A V_{ij}}_{H_c} + \underbrace{\frac{p_x^2}{2\mu_x} + \frac{p_y^2}{2\mu_y} + V_{v_1 v_2}}_{H_3} + \underbrace{\sum_{i=1}^A (V_{iv_1} + V_{iv_2})}_{H_{coup}}$$

$$\Psi = \mathcal{A} \{ \Phi_c(\{\vec{r}_A\}) \psi_3(\vec{r}_{v_1}, \vec{r}_{v_2}) \}$$

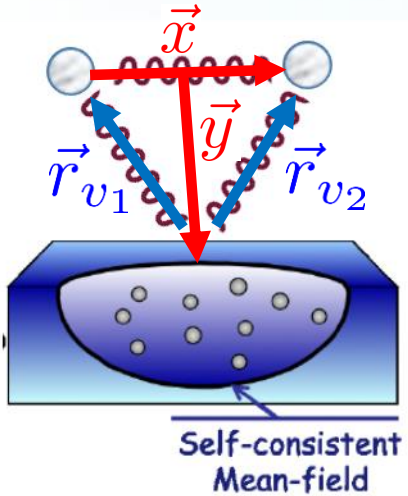
$$\langle \Psi | H' | \Psi \rangle = \langle \Psi | H | \Psi \rangle - E_c \int |\Phi_c(\{\vec{r}_A\})|^2 d\vec{r}_1 \cdots d\vec{r}_A - E_3 \int |\psi_3(\vec{r}_{v_1}, \vec{r}_{v_2})|^2 d\vec{r}_{v_1} d\vec{r}_{v_2}$$

$$0 = \frac{\delta}{\delta \Phi_c^*} \langle \Psi | H' | \Psi \rangle$$

$$0 = \frac{\delta}{\delta \psi_3^*} \langle \Psi | H' | \Psi \rangle$$

$$\Phi_c(\{\vec{r}_A\}) = \det(\{\phi_i^{q_i}(\vec{r}_i)\})$$

Formalism:



$$\begin{aligned}
 \epsilon_i \phi_i^{q_i}(\vec{r}) = & -\frac{\hbar^2}{2mA} \sum_{k=1}^A \int \phi_k^{q_k^*}(\vec{r}') \left(\vec{\nabla}_r - \vec{\nabla}_{r'} \right)^2 \left(\phi_k^{q_k}(\vec{r}') \phi_i^{q_i}(\vec{r}) - \phi_k^{q_k}(\vec{r}) \phi_i^{q_i}(\vec{r}') \delta_{q_i q_k} \right) d\vec{r}' \\
 & + \sum_{k=1}^A \int \phi_k^{q_k^*}(\vec{r}') V_{ik}(\vec{r}, \vec{r}') \left(\phi_k^{q_k}(\vec{r}') \phi_i^{q_i}(\vec{r}) - \phi_k^{q_k}(\vec{r}) \phi_i^{q_i}(\vec{r}') \delta_{q_i q_k} \right) d\vec{r}' \\
 & + \int \psi_3^*(\vec{r}_{v_1}, \vec{r}_{v_2}) V_{v_1 i}(\vec{r}_{v_1}, \vec{r}) \left(\psi_3(\vec{r}_{v_1}, \vec{r}_{v_2}) \phi_i^{q_i}(\vec{r}) - \psi_3(\vec{r}, \vec{r}_{v_2}) \phi_i^{q_i}(\vec{r}_{v_1}) \delta_{q_i q_{v_1}} \right) d\vec{r}_{v_1} d\vec{r}_{v_2} \\
 & + \int \psi_3^*(\vec{r}_{v_1}, \vec{r}_{v_2}) V_{v_2 i}(\vec{r}_{v_2}, \vec{r}) \left(\psi_3(\vec{r}_{v_1}, \vec{r}_{v_2}) \phi_i^{q_i}(\vec{r}) - \psi_3(\vec{r}_{v_1}, \vec{r}) \phi_i^{q_i}(\vec{r}_{v_2}) \delta_{q_i q_{v_2}} \right) d\vec{r}_{v_1} d\vec{r}_{v_2}
 \end{aligned}$$

$$\begin{aligned}
 E_3 \psi_3(\vec{r}_{v_1}, \vec{r}_{v_2}) = & \left(\frac{p_x^2}{2\mu_x} + \frac{p_y^2}{2\mu_y} + V_{v_1 v_2} \right) \psi_3(\vec{r}_{v_1}, \vec{r}_{v_2}) \\
 & + \sum_{i=1}^A \int \phi_i^{q_i^*}(\vec{r}) V_{v_1 i}(\vec{r}_{v_1}, \vec{r}) \left(\psi_3(\vec{r}_{v_1}, \vec{r}_{v_2}) \phi_i^{q_i}(\vec{r}) - \psi_3(\vec{r}, \vec{r}_{v_2}) \phi_i^{q_i}(\vec{r}_{v_1}) \delta_{q_{v_1} q_i} \right) d\vec{r} \\
 & + \sum_{i=1}^A \int \phi_i^{q_i^*}(\vec{r}) V_{v_2 i}(\vec{r}_{v_2}, \vec{r}) \left(\psi_3(\vec{r}_{v_1}, \vec{r}_{v_2}) \phi_i^{q_i}(\vec{r}) - \psi_3(\vec{r}_{v_1}, \vec{r}) \phi_i^{q_i}(\vec{r}_{v_2}) \delta_{q_{v_2} q_i} \right) d\vec{r}
 \end{aligned}$$

concludes that the single-particle wave functions ϕ_i have to satisfy the following set of equations (see Appendix C):

$$\left[-\vec{\nabla} \cdot \frac{\hbar^2}{2m_q^*(\vec{r})} \vec{\nabla} + U_q(\vec{r}) + \vec{W}_q(\vec{r}) \cdot (-i)(\vec{\nabla} \times \vec{\sigma}) \right] \phi_i = e_i \phi_i, \quad (20)$$

where q stands for the charge of the single-particle state i . Equation (20) has the form of a local Schrödinger equation with an effective mass $m^*(\vec{r})$ which depends on the density only,

$$\frac{\hbar^2}{2m_q^*(\vec{r})} = \frac{\hbar^2}{2m} + \frac{1}{4}(t_1 + t_2) \rho + \frac{1}{8}(t_2 - t_1) \rho_q; \quad (21)$$

whereas, the potential $U(\vec{r})$ also depends on the kinetic energy density,

$$\begin{aligned} U_q(\vec{r}) = & t_0 \left[\left(1 + \frac{1}{2} x_0\right) \rho - \left(x_0 + \frac{1}{2}\right) \rho_q \right] + \frac{1}{4} t_3 (\rho^2 - \rho_q^2) \\ & - \frac{1}{8} (3t_1 - t_2) \nabla^2 \rho + \frac{1}{16} (3t_1 + t_2) \nabla^2 \rho_q + \frac{1}{4} (t_1 + t_2) \tau \\ & + \frac{1}{8} (t_2 - t_1) \tau_q - \frac{1}{2} W_0 (\vec{\nabla} \cdot \vec{J} + \vec{\nabla} \cdot \vec{J}_q) + \delta_{q, +\frac{1}{2}} V_C(\vec{r}). \end{aligned} \quad (22a)$$

The form factor \vec{W} of the one-body spin-orbit potential is

$$\vec{W}_q(\vec{r}) = \frac{1}{2} W_0 (\vec{\nabla} \rho + \vec{\nabla} \rho_q) + \frac{1}{8} (t_1 - t_2) \vec{J}_q(\vec{r}). \quad (22b)$$

$$\epsilon_i \phi_i^{q_i}(\vec{r}) = \left[-\vec{\nabla} \cdot \frac{\hbar^2}{2m_{q_i}^*(\vec{r})} \vec{\nabla} + U_{q_i}(\vec{r}) - i\vec{W}_{q_i}(\vec{r}) \cdot (\vec{\nabla} \times \vec{\sigma}) - \vec{\nabla} \cdot \frac{1}{m'_{q_i}(\vec{r})} \vec{\nabla} + U'_{q_i}(\vec{r}) - i\vec{W}'_{q_i}(\vec{r}) \cdot (\vec{\nabla} \times \vec{\sigma}) \right] \phi_i^{q_i}(\vec{r})$$

$$E_3 \psi_3(\vec{r}_1, \vec{r}_2) = \left[\frac{p_x^2}{2\mu_x} + \frac{p_y^2}{2\mu_y} + V_{v_1 v_2} + V_{cv_1}(\vec{r}_{cv_1}) + V_{cv_2}(\vec{r}_{cv_2}) \right] \psi_3(\vec{r}_1, \vec{r}_2)$$

630

D. VAUTHERIN

concludes that the single-particle wave functions ϕ_i have to satisfy the following set of equations (see Appendix C):

$$\left[-\vec{\nabla} \cdot \frac{\hbar^2}{2m_q^*(\vec{r})} \vec{\nabla} + U_q(\vec{r}) + \vec{W}_q(\vec{r}) \cdot (-i)(\vec{\nabla} \times \vec{\sigma}) \right] \phi_i = e_i \phi_i, \quad (20)$$

where q stands for the charge of the single-particle state i . Equation (20) has the form of a local Schrödinger equation with an effective mass $m^*(\vec{r})$ which depends on the density only,

$$\frac{\hbar^2}{2m_q^*(\vec{r})} = \frac{\hbar^2}{2m} + \frac{1}{4}(t_1 + t_2)\rho + \frac{1}{8}(t_2 - t_1)\rho_q; \quad (21)$$

whereas, the potential $U(\vec{r})$ also depends on the kinetic energy density,

$$U_q(\vec{r}) = t_0 \left[\left(1 + \frac{1}{2}x_0\right)\rho - \left(x_0 + \frac{1}{2}\right)\rho_q \right] + \frac{1}{4}t_3(\rho^2 - \rho_q^2) - \frac{1}{8}(3t_1 - t_2)\nabla^2\rho + \frac{1}{16}(3t_1 + t_2)\nabla^2\rho_q + \frac{1}{4}(t_1 + t_2)\tau + \frac{1}{8}(t_2 - t_1)\tau_q - \frac{1}{2}W_0(\vec{\nabla} \cdot \vec{J} + \vec{\nabla} \cdot \vec{J}_q) + \delta_{q, \pm \frac{1}{2}} V_C(\vec{r}). \quad (22a)$$

The form factor \vec{W} of the one-body spin-orbit potential is

$$\vec{W}_q(\vec{r}) = \frac{1}{2}W_0(\vec{\nabla}\rho + \vec{\nabla}\rho_q) + \frac{1}{8}(t_1 - t_2)\vec{J}_q(\vec{r}). \quad (22b)$$

$$\epsilon_i \phi_i^{q_i}(\vec{r}) = \left[-\vec{\nabla} \cdot \frac{\hbar^2}{2m_{q_i}^*(\vec{r})} \vec{\nabla} + U_{q_i}(\vec{r}) - i\vec{W}_{q_i}(\vec{r}) \cdot (\vec{\nabla} \times \vec{\sigma}) - \vec{\nabla} \cdot \frac{1}{m'_{q_i}(\vec{r})} \vec{\nabla} + U'_{q_i}(\vec{r}) - i\vec{W}'_{q_i}(\vec{r}) \cdot (\vec{\nabla} \times \vec{\sigma}) \right] \phi_i^{q_i}(\vec{r})$$

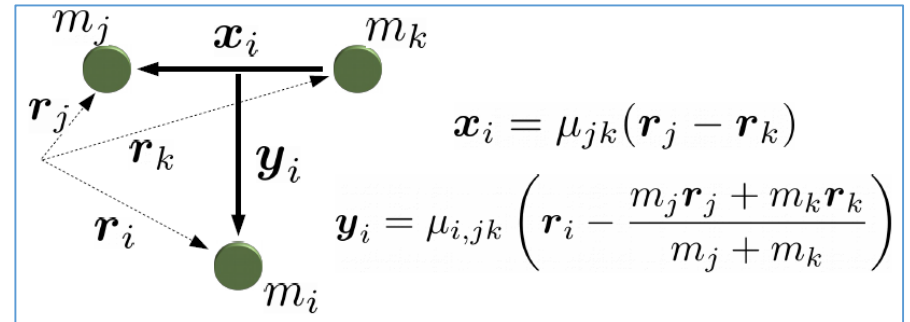
$$E_3 \psi_3(\vec{r}_1, \vec{r}_2) = \left[\frac{p_x^2}{2\mu_x} + \frac{p_y^2}{2\mu_y} + V_{v_1 v_2} + V_{cv_1}(\vec{r}_{cv_1}) + V_{cv_2}(\vec{r}_{cv_2}) \right] \psi_3(\vec{r}_1, \vec{r}_2)$$

Adiabatic Expansion Method

$$\psi_3(\vec{r}_{v_1}, \vec{r}_{v_2}) = \frac{1}{\rho^{5/2}} \sum_n f_n(\rho) \Phi_n(\rho, \Omega)$$

$$\rho^2 = x^2 + y^2 \quad \tan \alpha = \frac{x}{y}$$

$$\Omega \equiv \{ \alpha, \Omega_x, \Omega_y \}$$



630

D. VAUTHERIN

concludes that the single-particle wave functions ϕ_i have to satisfy the following set of equations (see Appendix C):

$$\left[-\vec{\nabla} \cdot \frac{\hbar^2}{2m_q^*(\vec{r})} \vec{\nabla} + U_q(\vec{r}) + \vec{W}_q(\vec{r}) \cdot (-i)(\vec{\nabla} \times \vec{\sigma}) \right] \phi_i = e_i \phi_i, \quad (20)$$

where q stands for the charge of the single-particle state i . Equation (20) has the form of a local Schrödinger equation with an effective mass $m^*(\vec{r})$ which depends on the density only,

$$\frac{\hbar^2}{2m_q^*(\vec{r})} = \frac{\hbar^2}{2m} + \frac{1}{4}(t_1 + t_2)\rho + \frac{1}{8}(t_2 - t_1)\rho_q; \quad (21)$$

whereas, the potential $U(\vec{r})$ also depends on the kinetic energy density,

$$U_q(\vec{r}) = t_0 \left[\left(1 + \frac{1}{2}x_0\right)\rho - \left(x_0 + \frac{1}{2}\right)\rho_q \right] + \frac{1}{4}t_3(\rho^2 - \rho_q^2) - \frac{1}{8}(3t_1 - t_2)\nabla^2\rho + \frac{1}{16}(3t_1 + t_2)\nabla^2\rho_q + \frac{1}{4}(t_1 + t_2)\tau + \frac{1}{8}(t_2 - t_1)\tau_q - \frac{1}{2}W_0(\vec{\nabla} \cdot \vec{J} + \vec{\nabla} \cdot \vec{J}_q) + \delta_{q, \pm\frac{1}{2}} V_C(\vec{r}). \quad (22a)$$

The form factor \vec{W} of the one-body spin-orbit potential is

$$\vec{W}_q(\vec{r}) = \frac{1}{2}W_0(\vec{\nabla}\rho + \vec{\nabla}\rho_q) + \frac{1}{8}(t_1 - t_2)\vec{J}_q(\vec{r}). \quad (22b)$$

$$\epsilon_i \phi_i^{q_i}(\vec{r}) = \left[-\vec{\nabla} \cdot \frac{\hbar^2}{2m_{q_i}^*(\vec{r})} \vec{\nabla} + U_{q_i}(\vec{r}) - i\vec{W}_{q_i}(\vec{r}) \cdot (\vec{\nabla} \times \vec{\sigma}) - \vec{\nabla} \cdot \frac{1}{m'_{q_i}(\vec{r})} \vec{\nabla} + U'_{q_i}(\vec{r}) - i\vec{W}'_{q_i}(\vec{r}) \cdot (\vec{\nabla} \times \vec{\sigma}) \right] \phi_i^{q_i}(\vec{r})$$

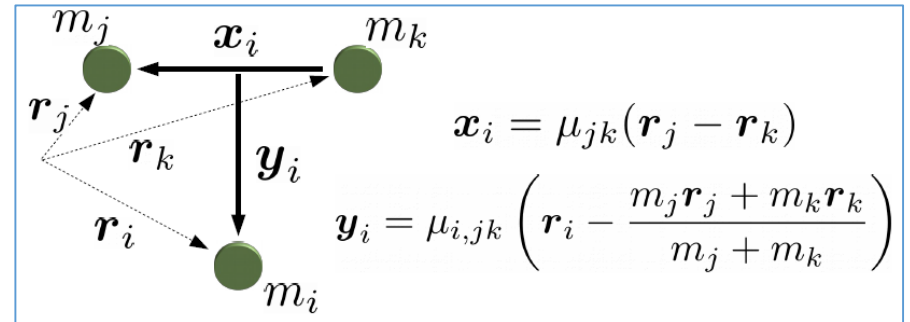
$$E_3 \psi_3(\vec{r}_1, \vec{r}_2) = \left[\frac{p_x^2}{2\mu_x} + \frac{p_y^2}{2\mu_y} + V_{v_1 v_2} + V_{cv_1}(\vec{r}_{cv_1}) + V_{cv_2}(\vec{r}_{cv_2}) \right] \psi_3(\vec{r}_1, \vec{r}_2)$$

Adiabatic Expansion Method

$$\psi_3(\vec{r}_{v_1}, \vec{r}_{v_2}) = \frac{1}{\rho^{5/2}} \sum_n f_n(\rho) \Phi_n(\rho, \Omega)$$

$$\rho^2 = x^2 + y^2 \quad \tan \alpha = \frac{x}{y}$$

$$\Omega \equiv \{ \alpha, \Omega_x, \Omega_y \}$$



$$\left[-\frac{\hbar^2}{2m} \frac{\partial^2}{\partial \rho^2} + V_{eff}(\rho) - E_3 \right] f_n - \frac{\hbar^2}{2m} \sum_m \left(2P_{nm}(\rho) \frac{\partial}{\partial \rho} + Q_{nm}(\rho) \right) f_m = 0$$

630

D. VAUTHERIN

concludes that the single-particle wave functions ϕ_i have to satisfy the following set of equations (see Appendix C):

$$\left[-\vec{\nabla} \cdot \frac{\hbar^2}{2m_q^*(\vec{r})} \vec{\nabla} + U_q(\vec{r}) + \vec{W}_q(\vec{r}) \cdot (-i)(\vec{\nabla} \times \vec{\sigma}) \right] \phi_i = e_i \phi_i, \quad (20)$$

where q stands for the charge of the single-particle state i . Equation (20) has the form of a local Schrödinger equation with an effective mass $m^*(\vec{r})$ which depends on the density only,

$$\frac{\hbar^2}{2m_q^*(\vec{r})} = \frac{\hbar^2}{2m} + \frac{1}{4}(t_1 + t_2)\rho + \frac{1}{8}(t_2 - t_1)\rho_q; \quad (21)$$

whereas, the potential $U(\vec{r})$ also depends on the kinetic energy density,

$$U_q(\vec{r}) = t_0 \left[\left(1 + \frac{1}{2}x_0\right)\rho - \left(x_0 + \frac{1}{2}\right)\rho_q \right] + \frac{1}{4}t_3(\rho^2 - \rho_q^2) - \frac{1}{8}(3t_1 - t_2)\nabla^2\rho + \frac{1}{16}(3t_1 + t_2)\nabla^2\rho_q + \frac{1}{4}(t_1 + t_2)\tau + \frac{1}{8}(t_2 - t_1)\tau_q - \frac{1}{2}W_0(\vec{\nabla} \cdot \vec{J} + \vec{\nabla} \cdot \vec{J}_q) + \delta_{q, \pm \frac{1}{2}} V_C(\vec{r}). \quad (22a)$$

The form factor \vec{W} of the one-body spin-orbit potential is

$$\vec{W}_q(\vec{r}) = \frac{1}{2}W_0(\vec{\nabla}\rho + \vec{\nabla}\rho_q) + \frac{1}{8}(t_1 - t_2)\vec{J}_q(\vec{r}). \quad (22b)$$

$$\epsilon_i \phi_i^{q_i}(\vec{r}) = \left[-\vec{\nabla} \cdot \frac{\hbar^2}{2m_{q_i}^*(\vec{r})} \vec{\nabla} + U_{q_i}(\vec{r}) - i\vec{W}_{q_i}(\vec{r}) \cdot (\vec{\nabla} \times \vec{\sigma}) - \vec{\nabla} \cdot \frac{1}{m'_{q_i}(\vec{r})} \vec{\nabla} + U'_{q_i}(\vec{r}) - i\vec{W}'_{q_i}(\vec{r}) \cdot (\vec{\nabla} \times \vec{\sigma}) \right] \phi_i^{q_i}(\vec{r})$$

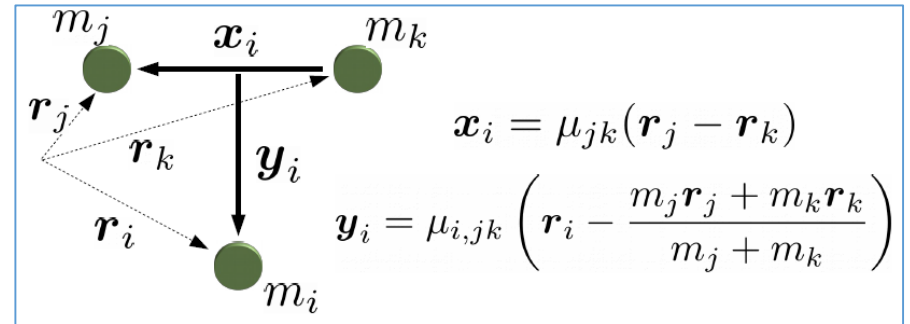
$$E_3 \psi_3(\vec{r}_1, \vec{r}_2) = \left[\frac{p_x^2}{2\mu_x} + \frac{p_y^2}{2\mu_y} + V_{v_1 v_2} + V_{cv_1}(\vec{r}_{cv_1}) + V_{cv_2}(\vec{r}_{cv_2}) \right] \psi_3(\vec{r}_1, \vec{r}_2)$$

Adiabatic Expansion Method

$$\psi_3(\vec{r}_{v_1}, \vec{r}_{v_2}) = \frac{1}{\rho^{5/2}} \sum_n f_n(\rho) \Phi_n(\rho, \Omega)$$

$$\rho^2 = x^2 + y^2 \quad \tan \alpha = \frac{x}{y}$$

$$\Omega \equiv \{ \alpha, \Omega_x, \Omega_y \}$$



D. Hove et al., JPG 45, 073001 (2018)

$$\left[-\frac{\hbar^2}{2m} \frac{\partial^2}{\partial \rho^2} + V_{eff}(\rho) - E_3 \right] f_n$$

$$-\frac{\hbar^2}{2m} \sum_m \left(2(P_{nm}(\rho) + P'_{nm}(\rho)) \frac{\partial}{\partial \rho} + Q_{nm}(\rho) + Q'_{nm}(\rho) \right) f_m = 0$$

The case of ^{26}O :

PRL 109, 022501 (2012)

PHYSICAL REVIEW LETTERS

week ending
13 JULY 2012

$N = 16$ Spherical Shell Closure in ^{24}O

K. Tshoo,^{1,*} Y. Satou,¹ H. Bhang,¹ S. Choi,¹ T. Nakamura,² Y. Kondo,² S. Deguchi,² Y. Kawada,² N. Kobayashi,² Y. Nakayama,² K. N. Tanaka,² N. Tanaka,² N. Aoi,³ M. Ishihara,³ T. Motobayashi,³ H. Otsu,³ H. Sakurai,³ S. Takeuchi,³ Y. Togano,³ K. Yoneda,³ Z. H. Li,³ F. Delaunay,⁴ J. Gibelin,⁴ F. M. Marqués,⁴ N. A. Orr,⁴ T. Honda,⁵ M. Matsushita,⁵ T. Kobayashi,⁶ Y. Miyashita,⁷ T. Sumikama,⁷ K. Yoshinaga,⁷ S. Shimoura,⁸ D. Sohler,⁹ T. Zheng,¹⁰ and Z. X. Cao¹⁰

¹Department of Physics and Astronomy, Seoul National University, Seoul 151-742, Korea

²Department of Physics, Tokyo Institute of Technology, Tokyo 152-8551, Japan

³RIKEN Nishina Center, Saitama 351-0198, Japan

⁴LPC-Caen, ENSICAEN, Université de Caen, CNRS/IN2P3, 14050 Caen Cedex, France

⁵Department of Physics, Rikkyo University, Tokyo 171-8501, Japan

⁶Department of Physics, Tohoku University, Aoba, Sendai, Miyagi 980-8578, Japan

⁷Department of Physics, Tokyo University of Science, Noda, Chiba 278-8510, Japan

⁸Center for Nuclear Study, University of Tokyo, Saitama 351-0198, Japan

⁹Institute of Nuclear Research of the Hungarian Academy of Sciences, P.O. Box 51, H-4001 Debrecen, Hungary

¹⁰School of Physics and State Key Laboratory of Nuclear Physics and Technology, Peking University, Beijing 100871, China

(Received 27 February 2012; published 12 July 2012)

The unbound excited states of the neutron drip-line isotope ^{24}O have been investigated via the $^{24}\text{O}(p, p')^{23}\text{O} + n$ reaction in inverse kinematics at a beam energy of 62 MeV/nucleon. The decay energy spectrum of $^{24}\text{O}^*$ was reconstructed from the momenta of ^{23}O and the neutron. The spin parity of the first excited state, observed at $E_x = 4.65 \pm 0.14$ MeV, was determined to be $J^\pi = 2^+$ from the angular distribution of the cross section. Higher-lying states were also observed. The quadrupole transition parameter β_2 of the 2^+ state was deduced, for the first time, to be 0.15 ± 0.04 . The relatively high excitation energy and small β_2 value are indicative of the $N = 16$ shell closure in ^{24}O .

Physics Letters B 672 (2009) 17–21



Contents lists available at ScienceDirect

Physics Letters B

www.elsevier.com/locate/physletb



Evidence for a doubly magic ^{24}O

C.R. Hoffman^{a,*}, I. Baumann^a, D. Bazin^b, J. Brown^c, G. Christian^{b,d}, D.H. Denby^e, P.A. DeYoung^e, J.E. Finck^f, N. Frank^{b,d,1}, J. Hinnefeld^g, S. Mosby^h, W.A. Peters^{b,d,2}, W.F. Rogers^h, A. Schiller^{b,3}, A. Spyrou^b, M.J. Scott^f, S.L. Tabor^a, M. Thoennessen^{b,d}, P. Voss^f

^aDepartment of Physics, Florida State University, Tallahassee, FL 32303, USA

^bNational Superconducting Cyclotron Laboratory, Michigan State University, East Lansing, MI 48824, USA

^cDepartment of Physics, Wabash College, Crawfordsville, IN 47933, USA

^dDepartment of Physics & Astronomy, Michigan State University, East Lansing, MI 48824, USA

^eDepartment of Physics, Hope College, Holland, MI 49423, USA

^fDepartment of Physics, Central Michigan University, Mt. Pleasant, MI 48859, USA

^gDepartment of Physics & Astronomy, Indiana University at South Bend, South Bend, IN 46634, USA

^hDepartment of Physics, Westmont College, Santa Barbara, CA 93108, USA

ARTICLE INFO

Article history:

Received 28 August 2008

Received in revised form 13 November 2008

Accepted 30 December 2008

Available online 6 January 2009

Editor: D.F. Geesaman

ABSTRACT

The decay energy spectrum for neutron unbound states in ^{24}O ($Z = 8$, $N = 16$) has been observed for the first time. The resonance energy of the lowest lying state, interpreted as the 2^+ level, has been observed at a decay energy above 600 keV. The resulting excitation energy of the 2^+ level above 4.7 MeV, supplies strong evidence that ^{24}O is a doubly magic nucleus. The data is also consistent with the presence of a second excited state around 5.33 MeV which can be interpreted as the 1^+ level.

© 2009 Elsevier B.V. All rights reserved.

PACS:

^{24}O is, to a large extent, a spherical nucleus

The case of ^{26}O :

PRL 116, 102503 (2016)

PHYSICAL REVIEW LETTERS

week ending
11 MARCH 2016

Nucleus ^{26}O : A Barely Unbound System beyond the Drip Line

Y. Kondo,¹ T. Nakamura,¹ R. Tanaka,¹ R. Minakata,¹ S. Ogoshi,¹ N. A. Orr,² N. L. Achouri,² T. Aumann,^{3,4} H. Baba,⁵ F. Delaunay,² P. Doornenbal,⁵ N. Fukuda,⁵ J. Gibelin,² J. W. Hwang,⁶ N. Inabe,⁵ T. Isobe,⁵ D. Kameda,⁵ D. Kanno,¹ S. Kim,⁶ N. Kobayashi,¹ T. Kobayashi,⁷ T. Kubo,⁵ S. Leblond,² J. Lee,⁵ F. M. Marqués,² T. Motobayashi,⁵ D. Murai,⁸ T. Murakami,⁹ K. Muto,⁷ T. Nakashima,¹ N. Nakatsuka,⁹ A. Navin,¹⁰ S. Nishi,¹ H. Otsu,⁵ H. Sato,⁵ Y. Satou,⁶ Y. Shimizu,⁵ H. Suzuki,⁵ K. Takahashi,⁷ H. Takeda,⁵ S. Takeuchi,⁵ Y. Togano,^{4,1} A. G. Tuff,¹¹ M. Vandebrouck,¹² and K. Yoneda⁵

¹Department of Physics, Tokyo Institute of Technology, 2-12-1 O-okayama, Meguro, Tokyo 152-8551, Japan

²LPC Caen, ENSICAEN, Université de Caen, CNRS/IN2P3, F-14050 Caen, France

³Institut für Kernphysik, Technische Universität Darmstadt, D-64289 Darmstadt, Germany

⁴ExtreMe Matter Institute EMMI and Research Division, GSI Helmholtzzentrum für Schwerionenforschung GmbH, D-64291 Darmstadt, Germany

⁵RIKEN Nishina Center, Hirosawa 2-1, Wako, Saitama 351-0198, Japan

⁶Department of Physics and Astronomy, Seoul National University, 599 Gwanak, Seoul 151-742, Republic of Korea

⁷Department of Physics, Tohoku University, Miyagi 980-8578, Japan

⁸Department of Physics, Rikkyo University, Toshima, Tokyo 171-8501, Japan

⁹Department of Physics, Kyoto University, Kyoto 606-8502, Japan

¹⁰Grand Accélérateur National d'Ions Lourds (GANIL), CEA/DRF-CNRS/IN2P3, Bvd Henri Becquerel, 14076 Caen, France

¹¹Department of Physics, University of York, Heslington, York YO10 5DD, United Kingdom

¹²Institut de Physique Nucléaire, Université Paris-Sud, IN2P3-CNRS, Université de Paris Sud, F-91406 Orsay, France

(Received 27 August 2015; published 9 March 2016)

The unbound nucleus ^{26}O has been investigated using invariant-mass spectroscopy following one-proton removal reaction from a ^{27}F beam at 201 MeV/nucleon. The decay products, ^{24}O and two neutrons, were detected in coincidence using the newly commissioned SAMURAI spectrometer at the RIKEN Radioactive Isotope Beam Factory. The ^{26}O ground-state resonance was found to lie only $18 \pm 3(\text{stat}) \pm 4(\text{syst})$ keV above threshold. In addition, a higher lying level, which is most likely the first 2^+ state, was observed for the first time at $1.28_{-0.08}^{+0.11}$ MeV above threshold. Comparison with theoretical predictions suggests that three-nucleon forces, pf -shell intruder configurations, and the continuum are key elements to understanding the structure of the most neutron-rich oxygen isotopes beyond the drip line.

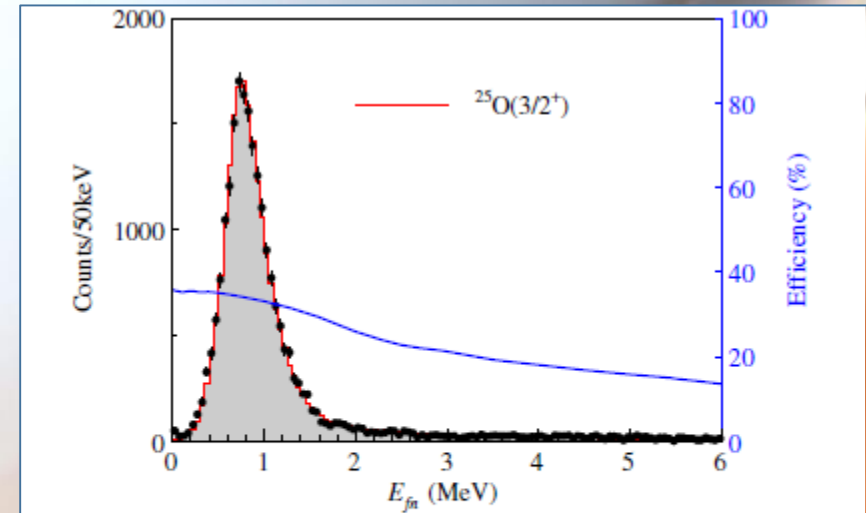
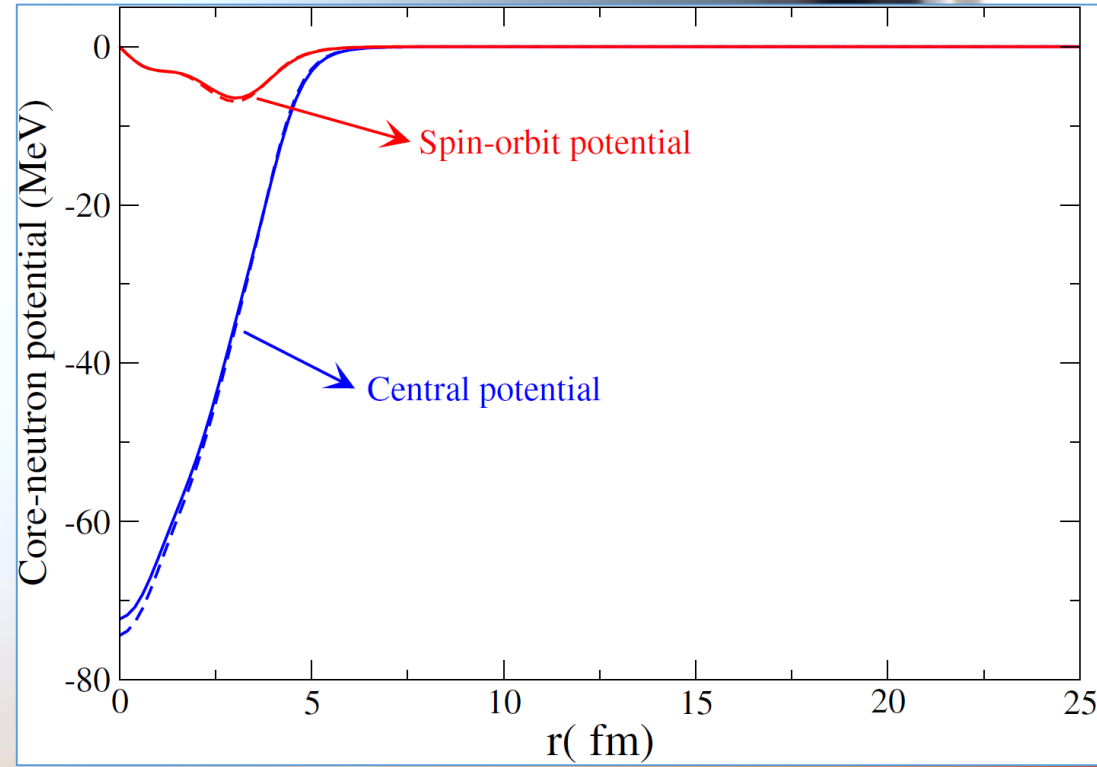
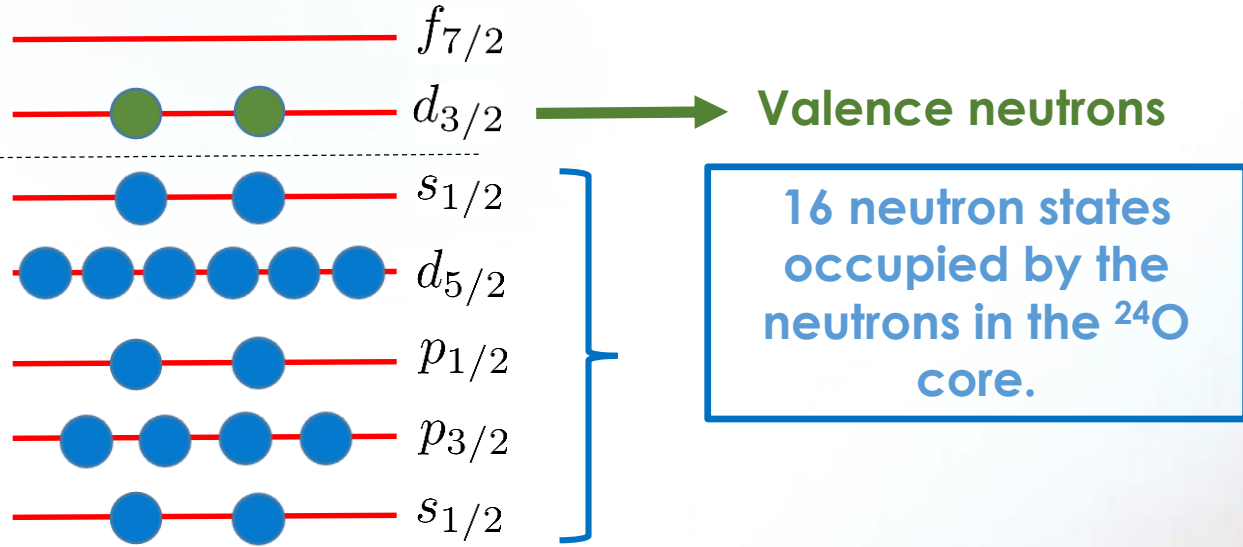


FIG. 1. Decay-energy spectrum of $^{24}\text{O} + n$ observed in one-proton removal from ^{26}F . The red-shaded histogram shows the fit, after accounting for the experimental response of the setup, assuming population of the ground state of ^{25}O . The blue curve represents the overall detection efficiency.

Experimental information about ^{26}O is available

The case of ^{26}O :



Adiabatic Expansion Method

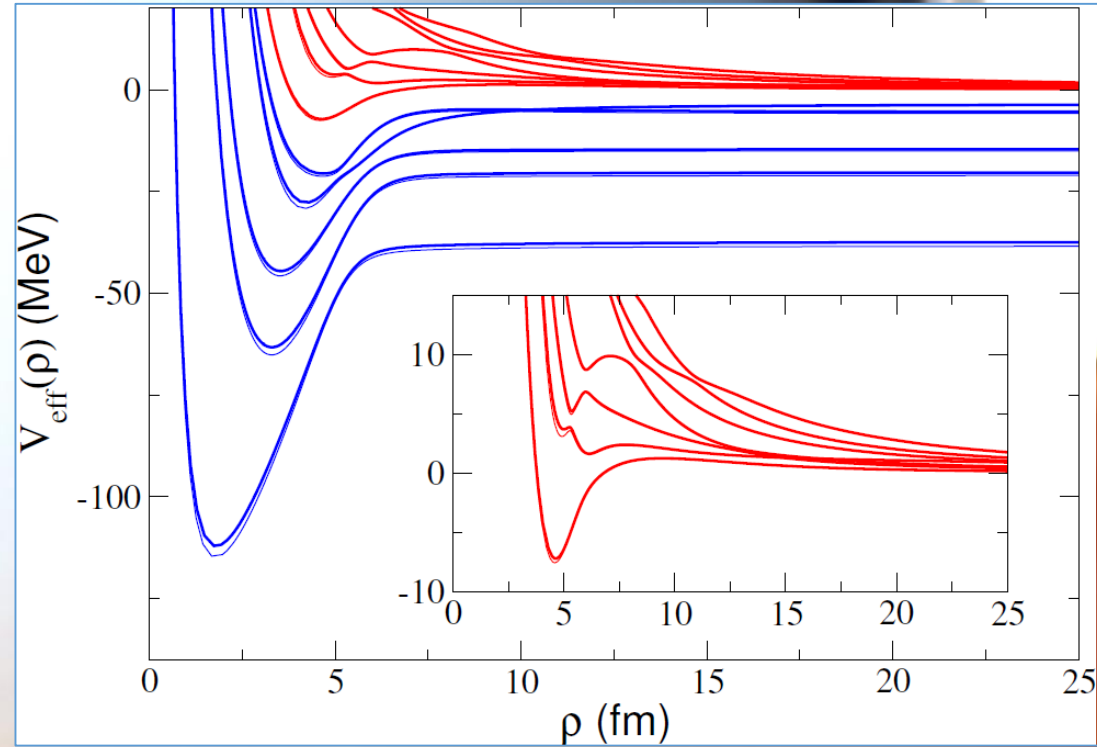
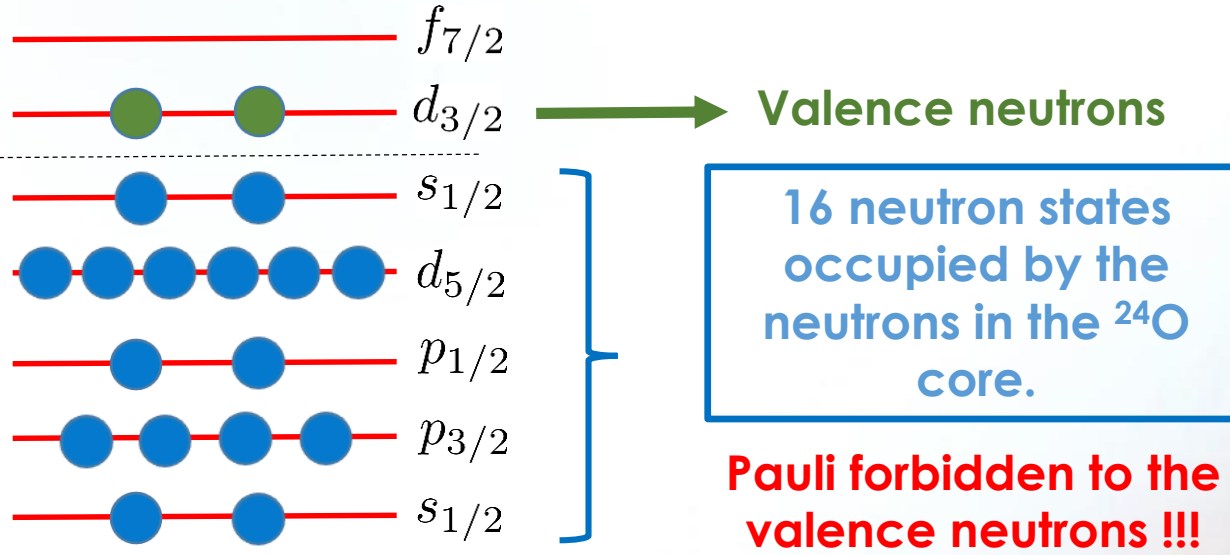
$$\psi_3(\vec{r}_{v_1}, \vec{r}_{v_2}) = \frac{1}{\rho^{5/2}} \sum_n f_n(\rho) \Phi_n(\rho, \Omega)$$

$$\left[-\frac{\hbar^2}{2m} \frac{\partial^2}{\partial \rho^2} + V_{eff}(\rho) - E_3 \right] f_n - \frac{\hbar^2}{2m} \sum_m \left(2P_{nm}(\rho) \frac{\partial}{\partial \rho} + Q_{nm}(\rho) \right) f_m = 0$$

	SLy4	SkM*	Sk3
$E_{d_{3/2}}$	0.85	0.83	1.23
$E_{d_{3/2}}(\text{HF})$	-0.96	-1.15	-0.53

s, p, d, and f waves are included in the calculation

The case of ^{26}O :



Adiabatic Expansion Method

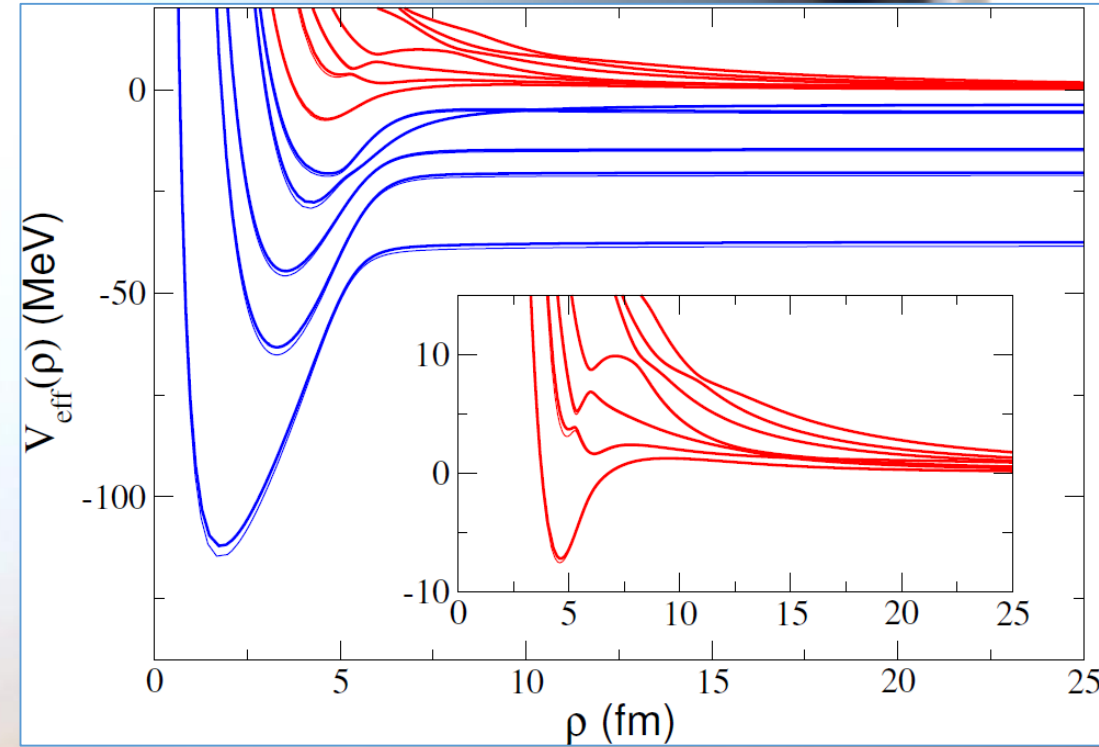
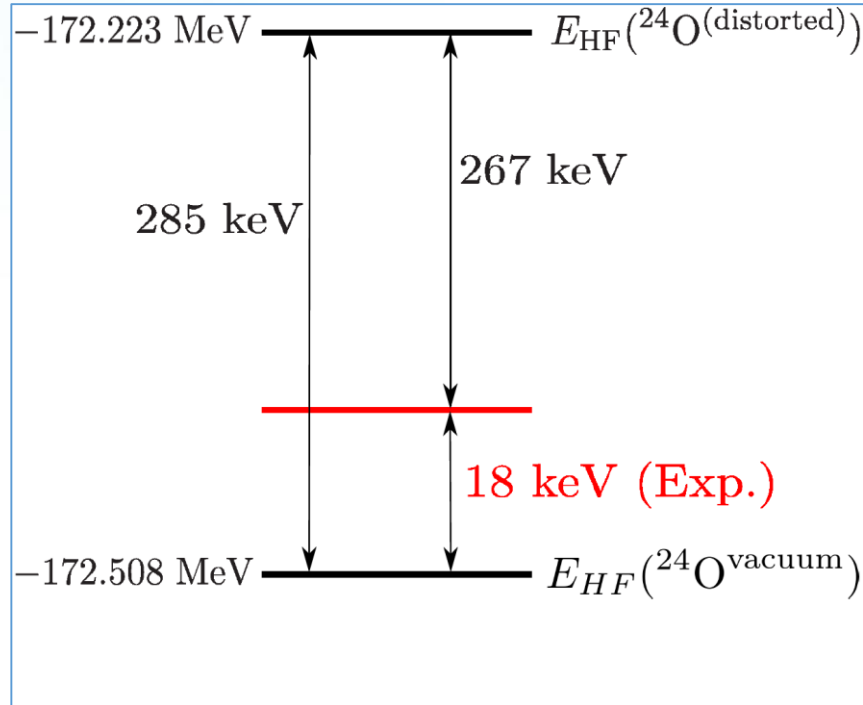
$$\psi_3(\vec{r}_{v_1}, \vec{r}_{v_2}) = \frac{1}{\rho^{5/2}} \sum_n f_n(\rho) \Phi_n(\rho, \Omega)$$

$$\left[-\frac{\hbar^2}{2m} \frac{\partial^2}{\partial \rho^2} + V_{\text{eff}}(\rho) - E_3 \right] f_n - \frac{\hbar^2}{2m} \sum_m \left(2P_{nm}(\rho) \frac{\partial}{\partial \rho} + Q_{nm}(\rho) \right) f_m = 0$$

The adiabatic channels associated to Pauli forbidden states are removed from the calculation

s , p , d , and f waves are included in the calculation

The case of ^{26}O :



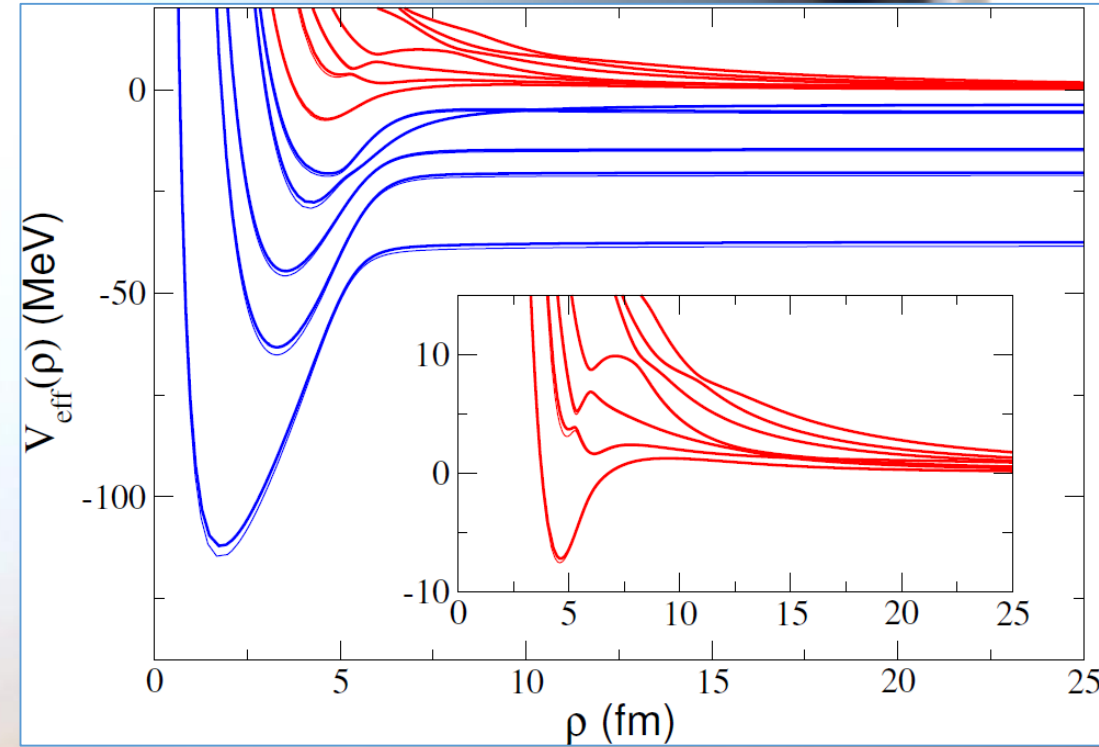
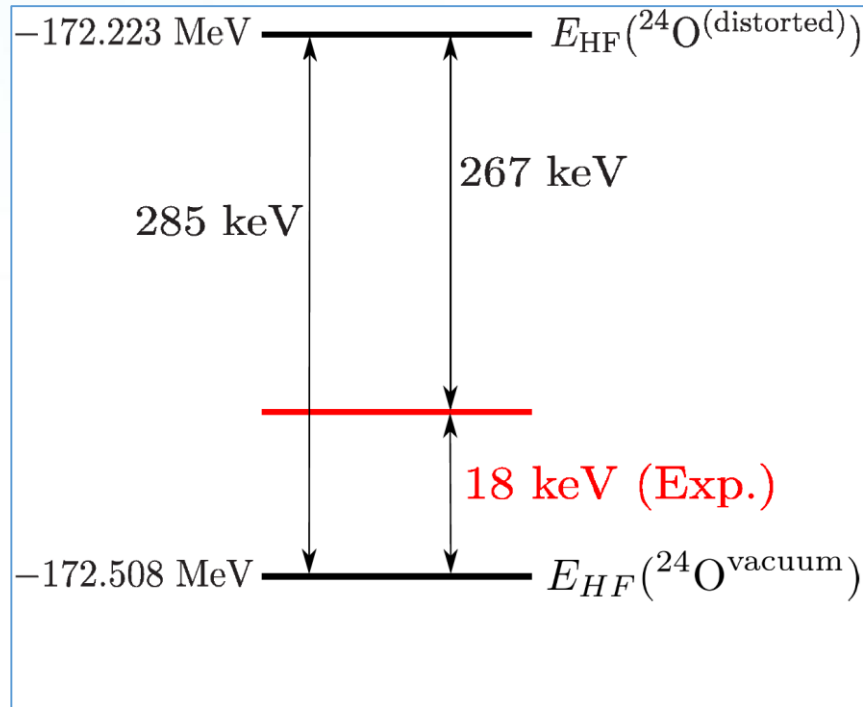
$$\left[-\frac{\hbar^2}{2m} \frac{\partial^2}{\partial \rho^2} + V_{\text{eff}}(\rho) + V_{3b}(\rho) - E_3 \right] f_n$$

$$-\frac{\hbar^2}{2m} \sum_m \left(2P_{nm}(\rho) \frac{\partial}{\partial \rho} + Q_{nm}(\rho) \right) f_m = 0$$

The adiabatic channels associated to Pauli forbidden states are removed from the calculation

s, p, d, and f waves are included in the calculation

The case of ^{26}O :



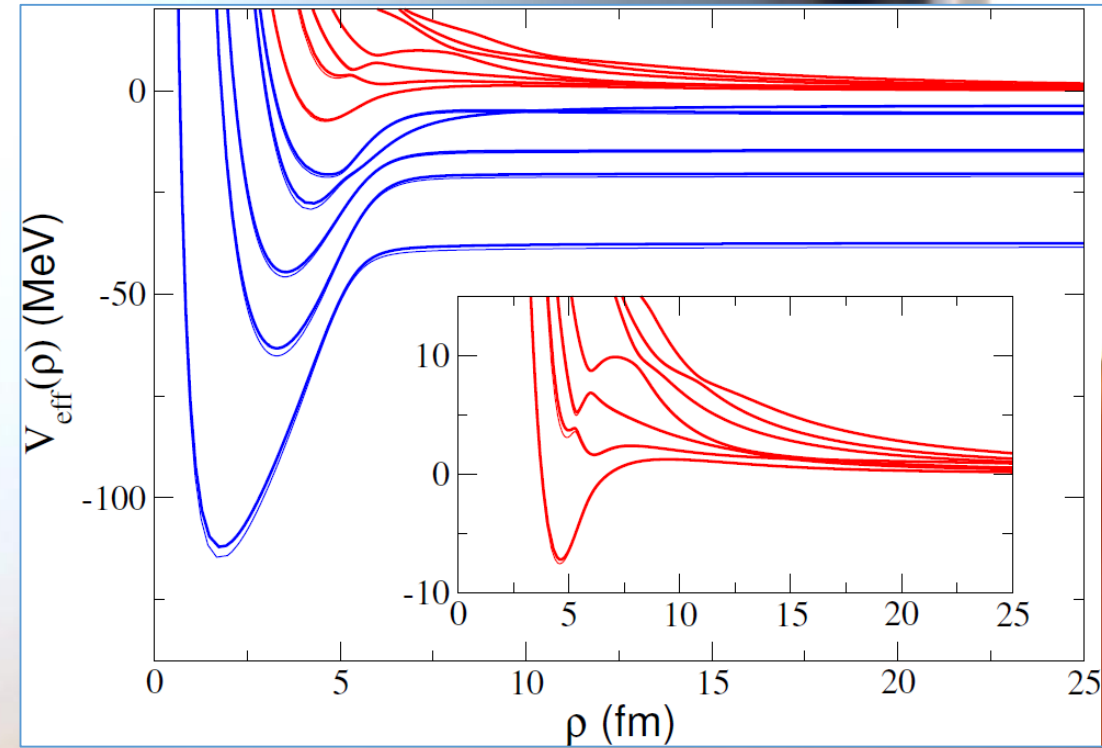
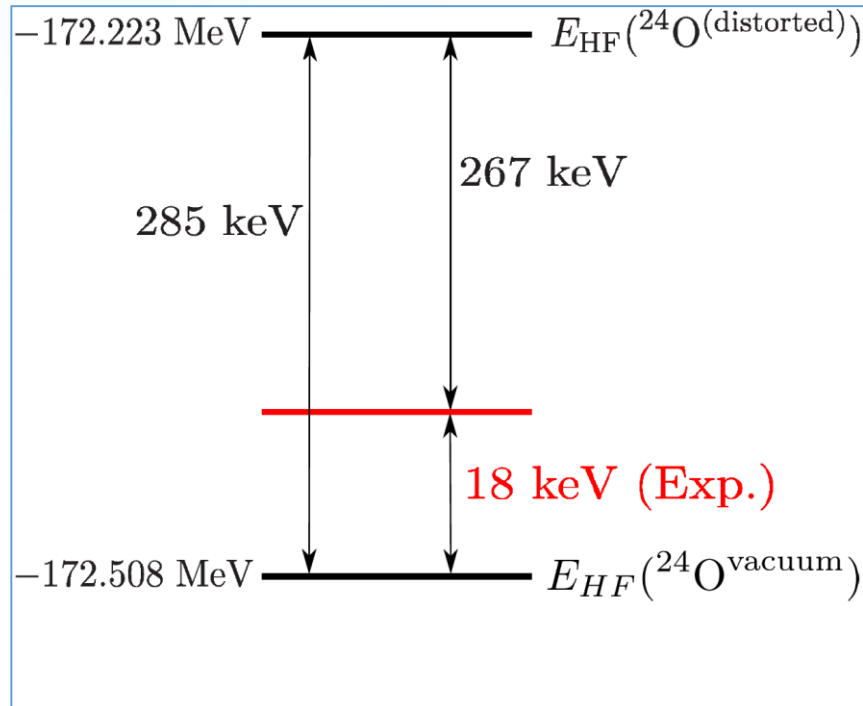
	$(d_{3/2}, d_{3/2})$	$(f_{7/2}, f_{7/2})$	$(p_{3/2}, p_{3/2})$
% of the norm	90.1	3.7	2.1

$$1 = \sum_{\ell_x} \int_0^\infty (|f_{\ell_x=0}(\rho)|^2 + |f_{\ell_x=1}(\rho)|^2 + |f_{\ell_x=2}(\rho)|^2 + \dots)$$

The adiabatic channels associated to Pauli forbidden states are removed from the calculation

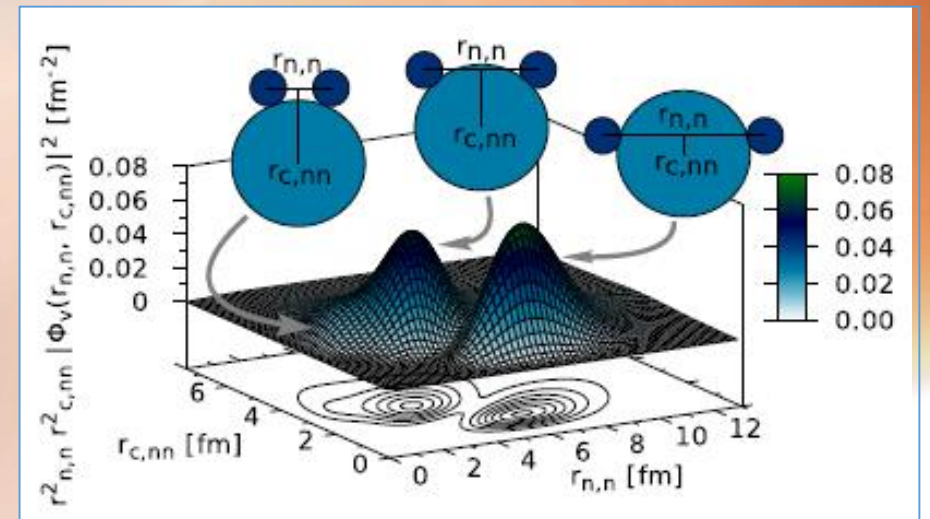
s, p, d, and f waves are included in the calculation

The case of ^{26}O :



	$(d_{3/2}, d_{3/2})$	$(f_{7/2}, f_{7/2})$	$(p_{3/2}, p_{3/2})$
% of the norm	90.1	3.7	2.1

$$1 = \sum_{\ell_x} \int_0^{\infty} (|f_{\ell_x=0}(\rho)|^2 + |f_{\ell_x=1}(\rho)|^2 + |f_{\ell_x=2}(\rho)|^2 + \dots)$$



The case of ^{26}O :

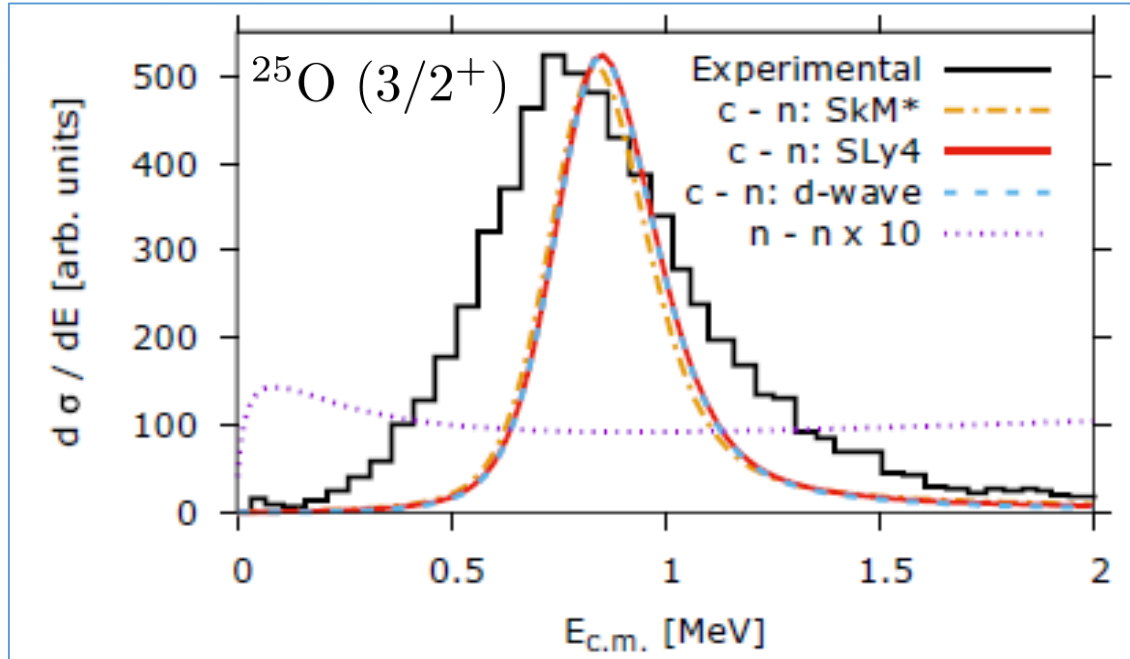
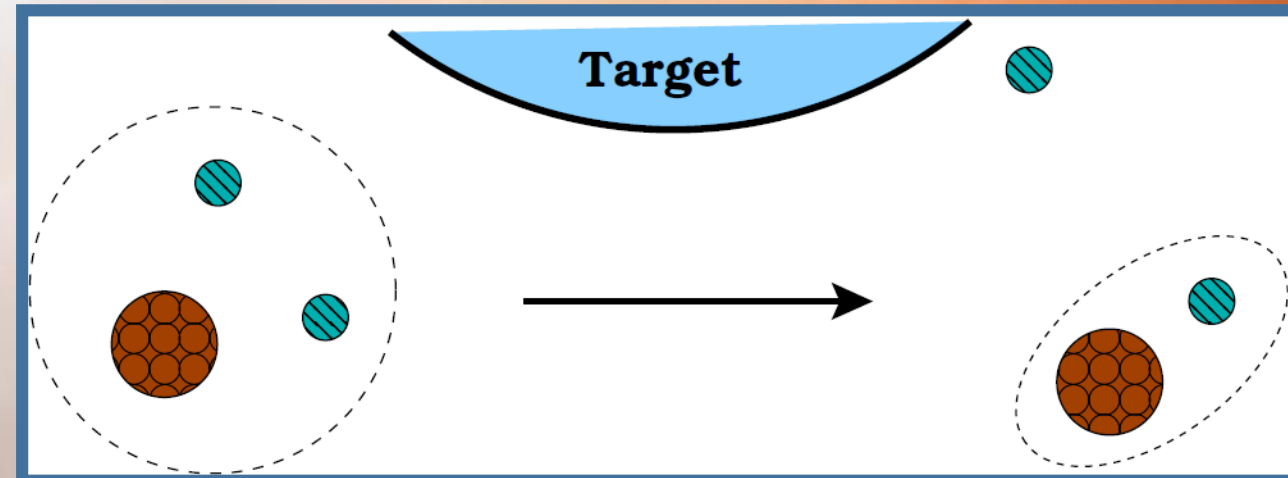


FIG. 4. The invariant mass spectra of core neutron for the SkM* (dash-dotted, orange) and SLy4 (solid, red) Skyrme parameters. The SLy4 core-neutron d -wave contribution (dashed, blue) and neutron-neutron (dotted, purple) invariant mass spectrum is also included. The black step curve is the measurements from Ref. [26].

Sudden approximation

$$\frac{d^6\sigma}{d\mathbf{k}_x d\mathbf{k}_y} \propto \sum_M \sum_{s_x \sigma_x \sigma_y} \left| \langle e^{i\mathbf{k}_x \cdot \mathbf{k}_y} \chi_{s_y}^{\sigma_y} w_{s_x}^{\sigma_x}(\mathbf{k}_x, x) | \Psi^{JM}(\mathbf{x}, \mathbf{y}) \rangle \right|^2$$

$$\frac{d\sigma}{dE_{nc}} = \frac{E_c E_n}{E_c + E_n} \frac{m(M_c + M_n)}{M_c M_n} \frac{1}{k_x} \frac{d\sigma}{dk_x}$$



The case of ^{26}O :

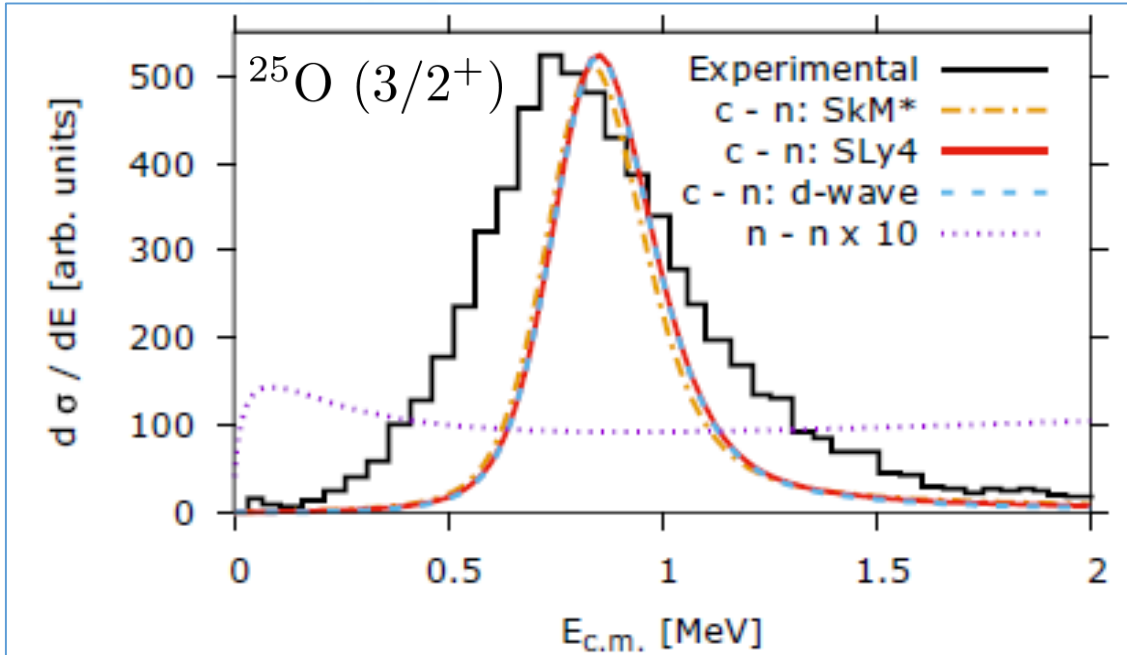


FIG. 4. The invariant mass spectra of core neutron for the SkM* (dash-dotted, orange) and SLy4 (solid, red) Skyrme parameters. The SLy4 core-neutron d -wave contribution (dashed, blue) and neutron-neutron (dotted, purple) invariant mass spectrum is also included. The black step curve is the measurements from Ref. [26].

Sudden approximation

$$\frac{d^6\sigma}{d\mathbf{k}_x d\mathbf{k}_y} \propto \sum_M \sum_{s_x \sigma_x \sigma_y} \left| \langle e^{i\mathbf{k}_x \cdot \mathbf{k}_y} \chi_{s_y}^{\sigma_y} w_{s_x}^{\sigma_x}(\mathbf{k}_x, x) | \Psi^{JM}(x, \mathbf{y}) \rangle \right|^2$$

$$\frac{d\sigma}{dE_{nc}} = \frac{E_c E_n}{E_c + E_n} \frac{m(M_c + M_n)}{M_c M_n} \frac{1}{k_x} \frac{d\sigma}{dk_x}$$

Once the NN interaction has been chosen, the invariant mass spectrum is fully determined.

Two-proton capture: ^{70}Kr

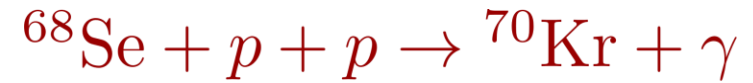
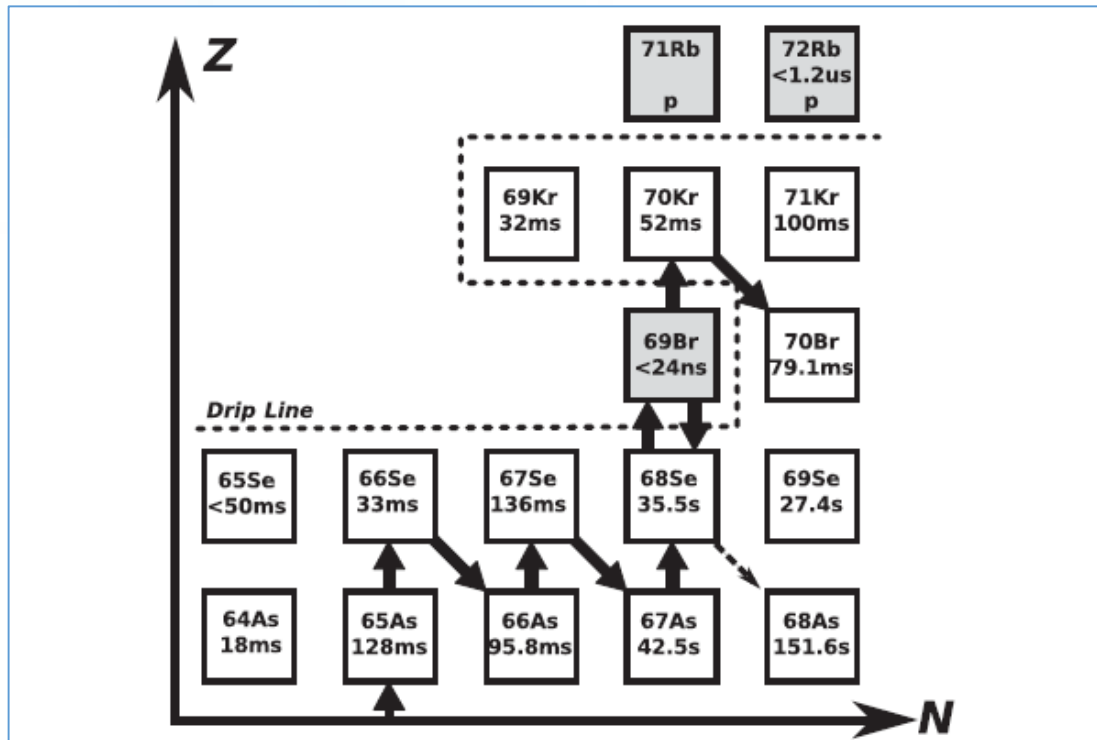


FIG. 1. Illustration of $2p$ -capture reactions through ^{69}Br bypassing the ^{68}Se waiting point. The slow β decay of ^{68}Se restricts the rp -process reaction flow in type I x-ray bursts.

Two-proton capture: ^{70}Kr

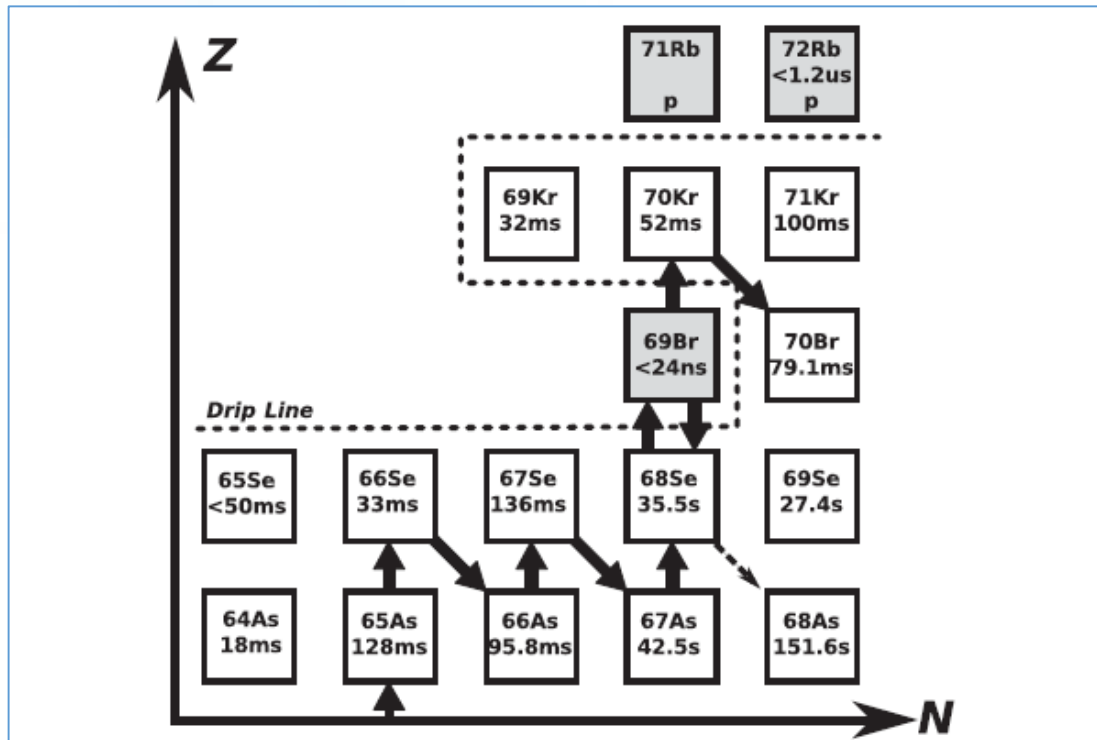
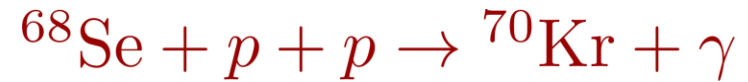


FIG. 1. Illustration of $2p$ -capture reactions through ^{69}Br by-passing the ^{68}Se waiting point. The slow β decay of ^{68}Se restricts the rp-process reaction flow in type I x-ray bursts.

A.M. Rogers et al., PRL 106, 252503 (2011)



$$R_{ppc}(E) = \frac{8\pi}{(\mu_{cp}\mu_{cp,p})^{3/2}} \frac{\hbar^3}{c^2} \left(\frac{E_\gamma}{E}\right)^2 \sigma_\gamma^\lambda(E_\gamma)$$

$$\sigma_\gamma^\lambda(E_\gamma) = \frac{(2\pi)^3(\lambda+1)}{\lambda((2\lambda+1)!!)^2} \left(\frac{E_\gamma}{\hbar c}\right)^{2\lambda-1} \frac{d}{dE} \mathcal{B}(E\lambda, 0^+ \rightarrow \lambda^\pi)$$

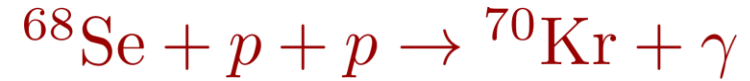
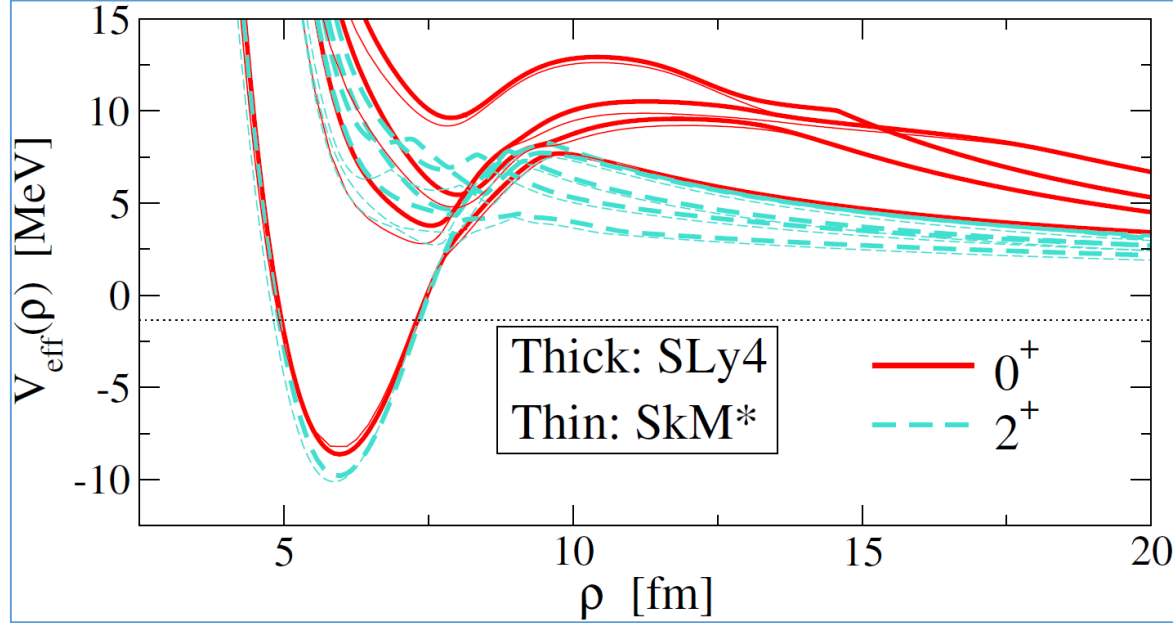
$$E_\gamma = E + |E_{g.s}|$$

$$\frac{d}{dE} \mathcal{B}(E\lambda, 0^+ \rightarrow \lambda^\pi) = \sum_i \left| \langle \psi_{\lambda^\pi}^{(i)} \parallel \hat{O}_\lambda \parallel \Psi_{0^+} \rangle \right|^2 \delta(E - E_i)$$

$$\langle R_{ppc}(E) \rangle = \frac{1}{2(KT)^3} \int E^2 R_{ppc}(E) e^{-E/KT} dE$$

✓ Dominated by the E2 transition $2^+ \rightarrow 0^+$

Two-proton capture: ^{70}Kr



$$R_{ppc}(E) = \frac{8\pi}{(\mu_{cp}\mu_{cp,p})^{3/2}} \frac{\hbar^3}{c^2} \left(\frac{E_\gamma}{E}\right)^2 \sigma_\gamma^\lambda(E_\gamma)$$

$$\sigma_\gamma^\lambda(E_\gamma) = \frac{(2\pi)^3(\lambda+1)}{\lambda((2\lambda+1)!!)^2} \left(\frac{E_\gamma}{\hbar c}\right)^{2\lambda-1} \frac{d}{dE} \mathcal{B}(E\lambda, 0^+ \rightarrow \lambda^\pi)$$

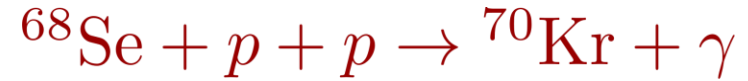
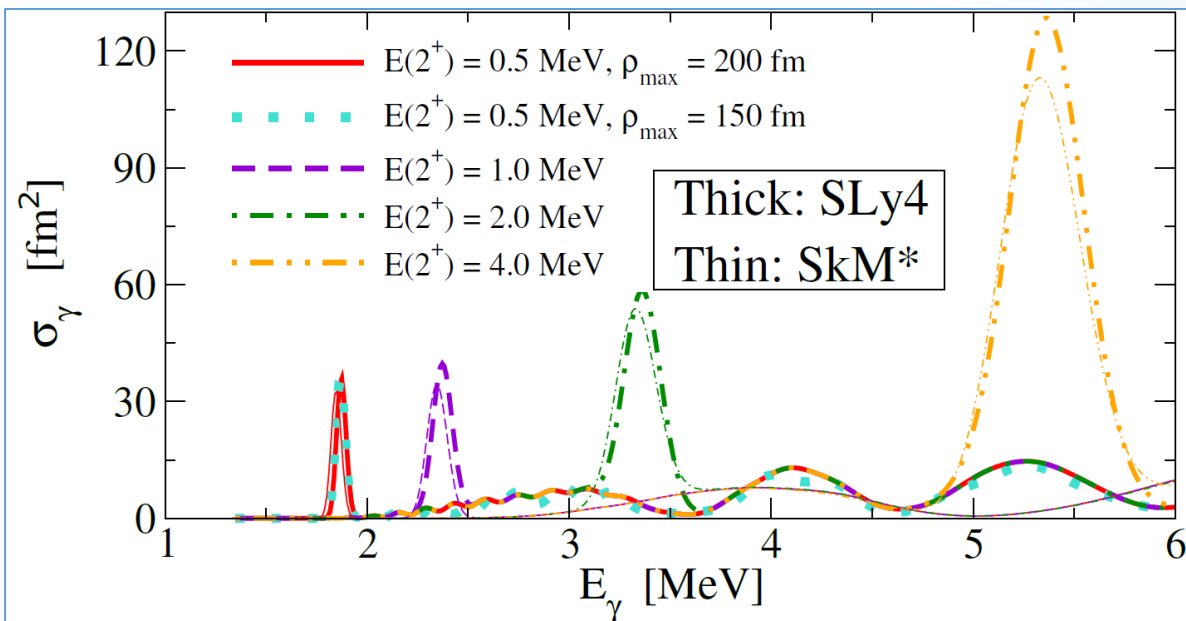
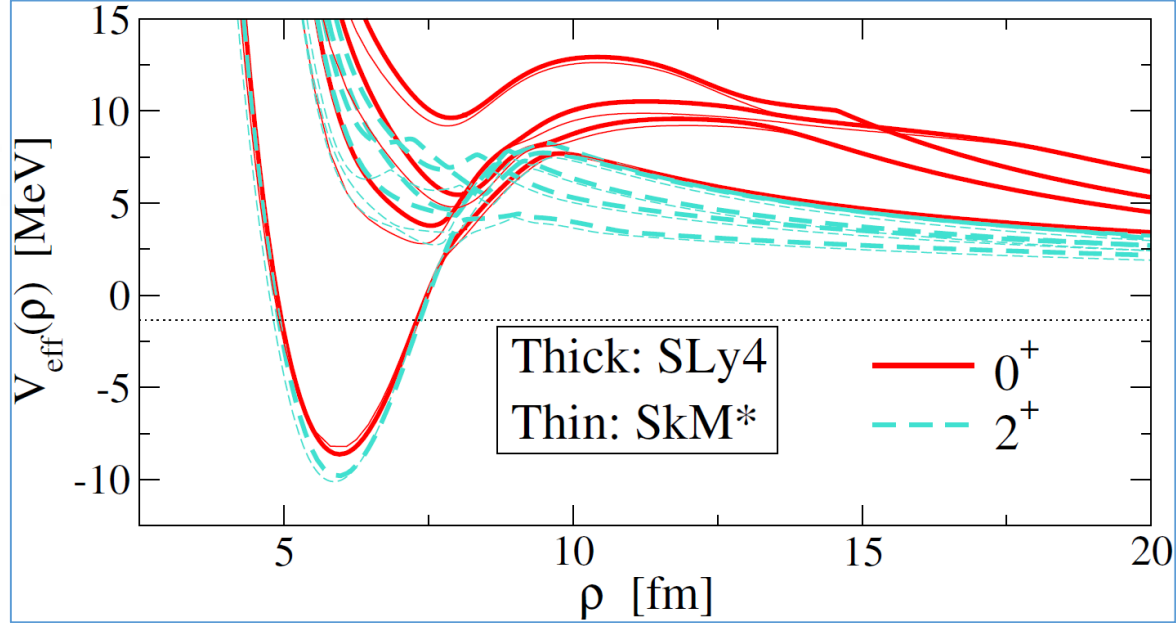
$$E_\gamma = E + |E_{g.s}|$$

$$\frac{d}{dE} \mathcal{B}(E\lambda, 0^+ \rightarrow \lambda^\pi) = \sum_i \left| \langle \psi_{\lambda^\pi}^{(i)} \parallel \hat{O}_\lambda \parallel \Psi_{0^+} \rangle \right|^2 \delta(E - E_i)$$

$$\langle R_{ppc}(E) \rangle = \frac{1}{2(KT)^3} \int E^2 R_{ppc}(E) e^{-E/KT} dE$$

✓ Dominated by the E2 transition $2^+ \rightarrow 0^+$

Two-proton capture: ^{70}Kr



$$R_{ppc}(E) = \frac{8\pi}{(\mu_{cp}\mu_{cp,p})^{3/2}} \frac{\hbar^3}{c^2} \left(\frac{E_\gamma}{E}\right)^2 \sigma_\gamma^\lambda(E_\gamma)$$

$$\sigma_\gamma^\lambda(E_\gamma) = \frac{(2\pi)^3(\lambda+1)}{\lambda((2\lambda+1)!!)^2} \left(\frac{E_\gamma}{\hbar c}\right)^{2\lambda-1} \frac{d}{dE} \mathcal{B}(E\lambda, 0^+ \rightarrow \lambda^\pi)$$

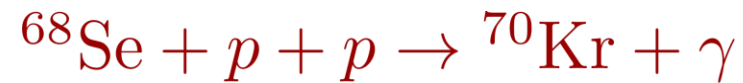
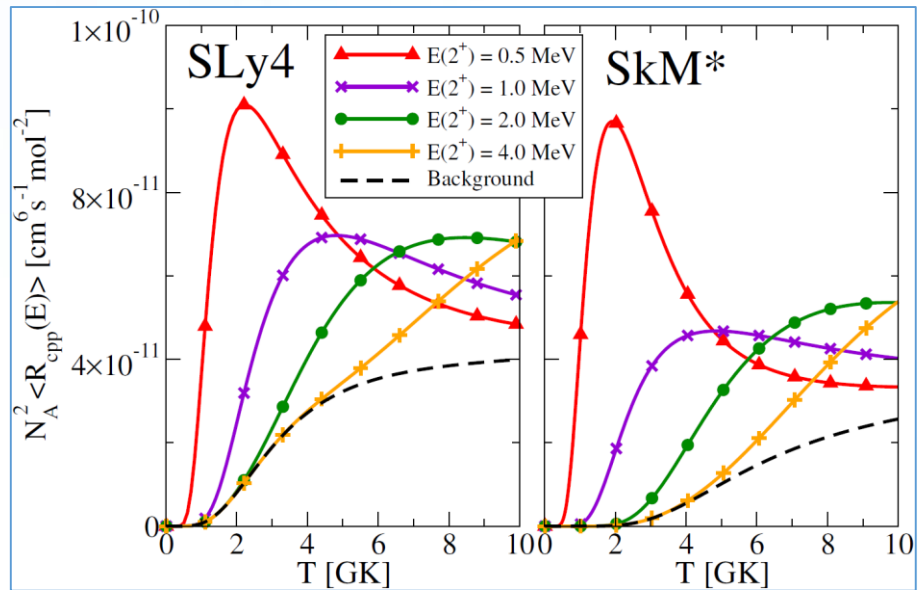
$$E_\gamma = E + |E_{g.s}|$$

$$\frac{d}{dE} \mathcal{B}(E\lambda, 0^+ \rightarrow \lambda^\pi) = \sum_i \left| \langle \psi_{\lambda^\pi}^{(i)} \parallel \hat{O}_\lambda \parallel \Psi_{0^+} \rangle \right|^2 \delta(E - E_i)$$

$$\langle R_{ppc}(E) \rangle = \frac{1}{2(KT)^3} \int E^2 R_{ppc}(E) e^{-E/KT} dE$$

✓ Dominated by the E2 transition $2^+ \rightarrow 0^+$

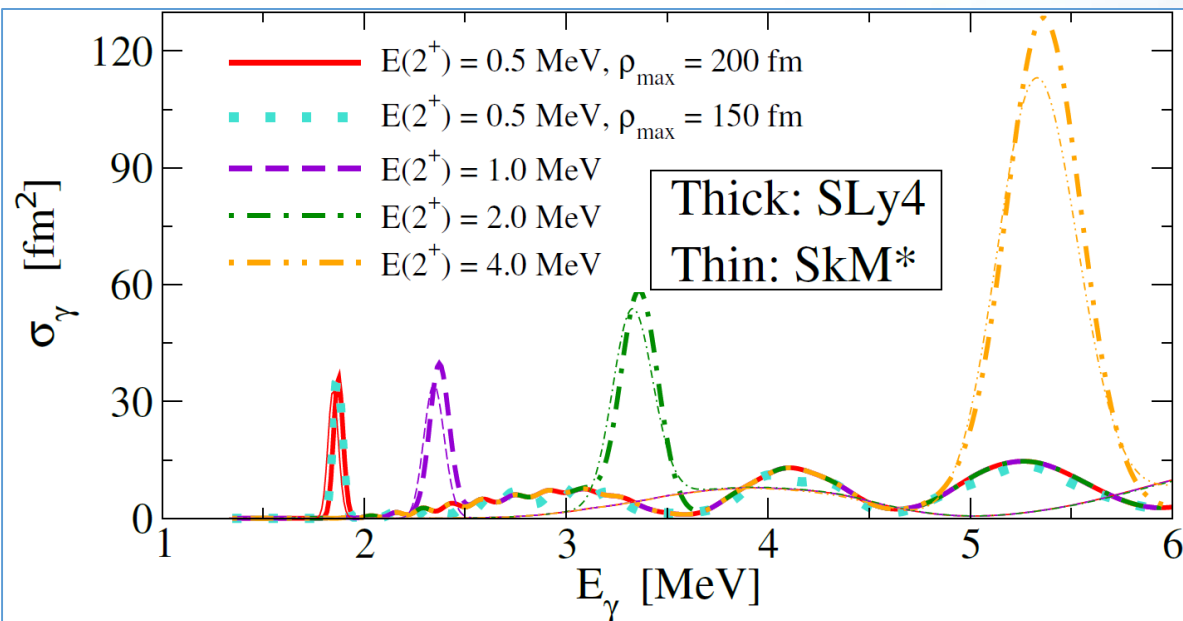
Two-proton capture: ^{70}Kr



$$R_{ppc}(E) = \frac{8\pi}{(\mu_{cp}\mu_{cp,p})^{3/2}} \frac{\hbar^3}{c^2} \left(\frac{E_\gamma}{E}\right)^2 \sigma_\gamma^\lambda(E_\gamma)$$

$$\sigma_\gamma^\lambda(E_\gamma) = \frac{(2\pi)^3(\lambda+1)}{\lambda((2\lambda+1)!!)^2} \left(\frac{E_\gamma}{\hbar c}\right)^{2\lambda-1} \frac{d}{dE} \mathcal{B}(E\lambda, 0^+ \rightarrow \lambda^\pi)$$

$$E_\gamma = E + |E_{g.s}|$$

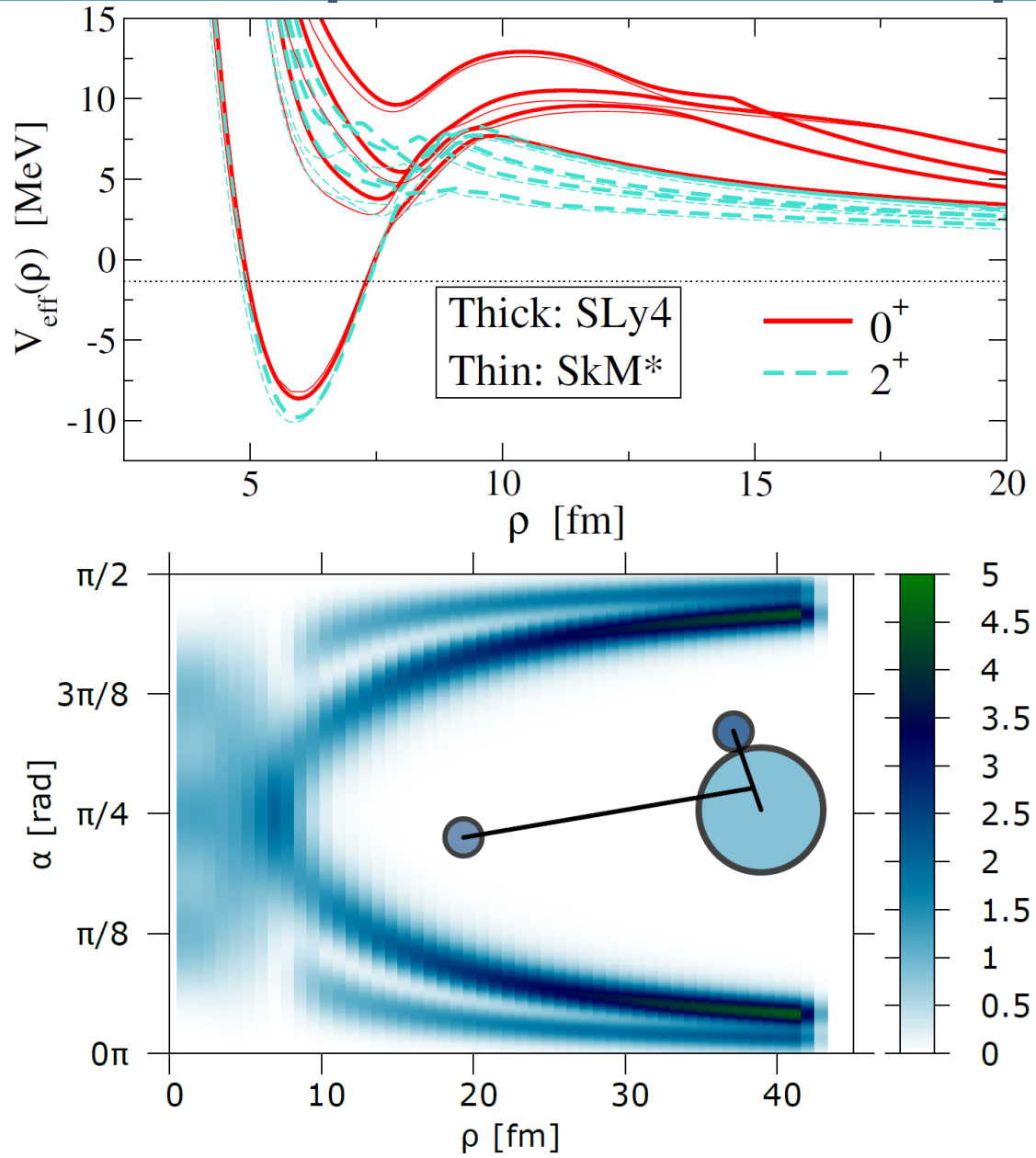


$$\frac{d}{dE} \mathcal{B}(E\lambda, 0^+ \rightarrow \lambda^\pi) = \sum_i \left| \langle \psi_{\lambda^\pi}^{(i)} \parallel \hat{O}_\lambda \parallel \Psi_{0^+} \rangle \right|^2 \delta(E - E_i)$$

$$\langle R_{ppc}(E) \rangle = \frac{1}{2(KT)^3} \int E^2 R_{ppc}(E) e^{-E/KT} dE$$

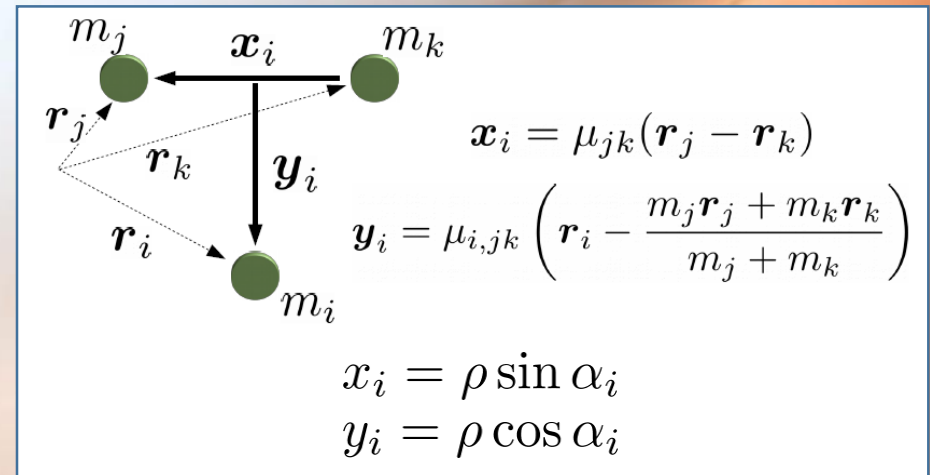
✓ Dominated by the E2 transition $2^+ \rightarrow 0^+$

Two-proton capture: ^{70}Kr



Capture mechanism

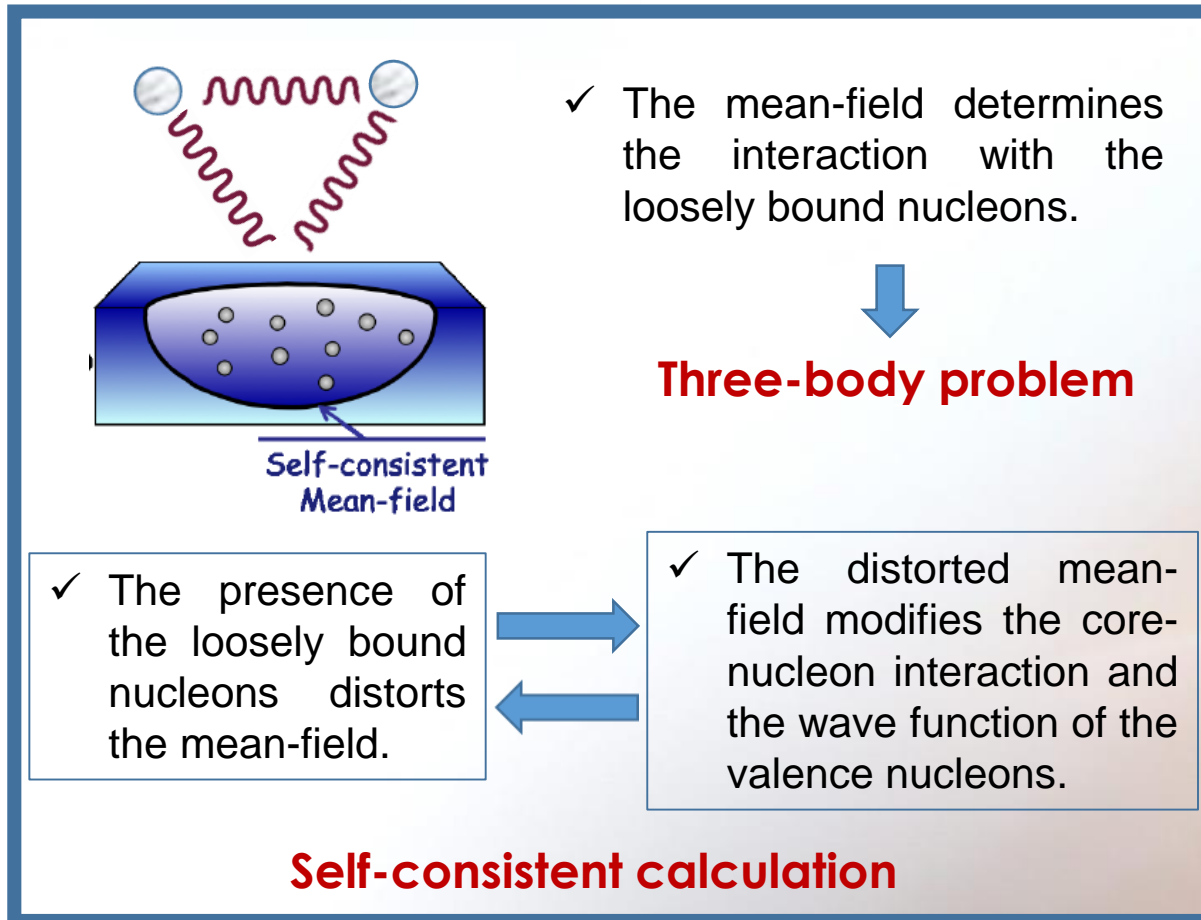
$$P(\alpha, \rho) = \sin^2 \alpha \cos^2 \alpha \int |\Phi(\rho, \alpha, \Omega_x, \Omega_y)|^2 d\Omega_x d\Omega_y$$



✓ Sequential capture through the $f_{5/2}$ resonance in ^{69}Br at 0.6 MeV.

Summary:

The model presented here treats the many-body core and the two valence particles self-consistently:



Core: Spherical Skyrme Hartree-Fock

- ✓ Core deformation?
- ✓ Finite range NN interactions?
- ✓ odd-odd nuclei?

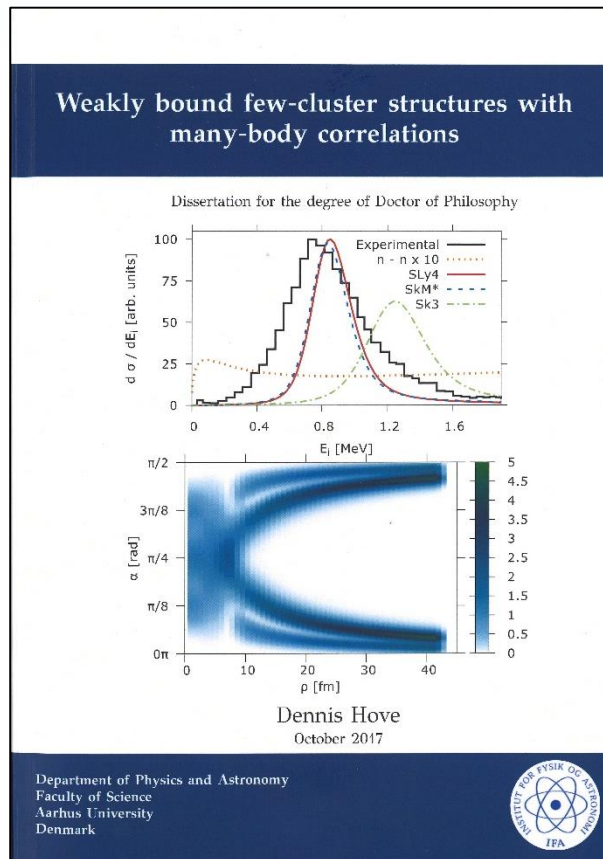
Three-body calculation: Adiabatic expansion

- ✓ Three-body force from the mean field?

- ✓ Generalization to more than one cluster and more than two valence nucleons

Weakly bound nuclei:

A unified description of intrinsic and relative degrees of freedom



Dennis Hove, Aksel S. Jensen
Aarhus University, Denmark



Pedro Sarriguren, Eduardo Garrido
IEM-CSIC, Madrid, Spain